Characterization of Electronic Structure in Molecules by One-Center Expansion Techniques. No Three-Center Four-Electron Bond in PF_5

Marco Häser

Contribution from the Institut für Physikalische Chemie, Universität Karlsruhe (TH), D-76128 Karlsruhe, Germany

Received September 11, 1995. Revised Manuscript Received May 24, 1996[⊗]

Abstract: The one-center expansion technique is applied to analyze the electronic structure of molecules in terms of angular momentum eigenfunctions (*s*, *p*, *d*, ...) of the participating atoms. That is, by scanning through a continuous set of spherical neighborhoods of a given atom, the surrounding molecular electronic structure is characterized by functions of radius from an otherwise unbiased atomic point of view. These functions include (a) radial densities/populations of angular momentum eigenfunctions, (b) their responses, e.g., to structural changes, and (c) the extent to which the one-particle density matrix can locally be described in terms of a preset number of "natural" orbitals (study of hypervalence). Covalence and delocalization, which by definition are not attributable to a single atom, are characterized by the degree of electron sharing between angular momentum eigenstates referring to different atomic neighborhoods. A concept of hybrid orbitals in chemical bonding with no other ingredients than principles of quantum mechanics and (spherical) atomic neighborhoods is outlined. The proposed approach is applicable to any approximation of electronic structure that allows the construction of a one-particle density operator in terms of an arbitrary one-particle basis set. Elementary applications to H_2, ethane, F_2, and benzene and a thorough analysis of the electronic structure of PF_5 are presented. The main results with respect to D_{3h}-symmetric PF_5 are the following: (a) a model of (spectroscopic) sp^3d hybrid orbitals at phosphorus is inappropriate; (b) a Rundle model with three two-center two-electron bonds and one three-center four-electron bond does not apply; (c) strong *3s* participation at P in covalent bonding with all five fluorine atoms creates different delocalization patterns instead; (d) a description of the valence region of phosphorus by only four orbitals is unsatisfactory (octet rule violation), and is best improved by an additional orbital of local *d* character; (e) the corresponding *d* population is only weakly bound to phosphorus, and should not be considered as chemically bonding.

I. Introduction

The electronic wave function of a molecule, as well as its response to perturbations (including changes in molecular structure), is the principal source of information about chemical bonds and about the characteristics of the atomic fragments which participate in them. Unfortunately, the latter entities are not observables that could unambiguously be represented by linear operators, let alone be measured experimentally. Nevertheless, most chemists will agree that the question whether two atoms A and B are linked by a $d_\pi-p_\pi$ bond is chemically meaningful.

Conventionally such information is retrieved from electronic wave functions by means of population analyses.[1−4] Common to the popular schemes is an empirical partitioning of the electronic one-particle density matrix into atomic and overlap contributions. A non-empirical partitioning of a molecule into atomic domains has been worked out by Bader,[5−7] but it necessitates certain extensions of the basic quantum mechanical postulates (subspace quantum mechanics) that are not universally accepted. A partitioning based on generalized atomic polar tensors has been proposed by Cioslowski.[8] Finally we want to mention Becke's electron localization function (ELF),[9] which beautifully condenses qualitative aspects of electronic (de-)localization into a single function in space.

Here we introduce another tool for analyzing molecular electronic wave functions in terms of characteristics of chemical bonding and of the participating atomic fragments. Our approach adheres to the following principles:

1. It is applicable to any type of electronic wave function, and in particular makes no reference to the type of basis set used, be it atom-centered functions, plane waves, etc.
2. There is no *a priori* partitioning into atomic domains.
3. All quantities used for a characterization of electronic structure are obtained non-empirically as expectation values of linear Hermitian operators.
4. Chemical concepts like valence, $d_\pi-p_\pi$ bonds, and delocalization will be accommodated.

We describe our approach in Sections II−IV, starting from known concepts like radial densities (Section II). We move on to the question of atomic valence (Section III), asking: How many orbitals are needed to describe electronic structure in *any* spherical atomic neighborhood? Finally we address covalence and delocalization (Section IV), and outline how the concept of hybrid orbitals in chemical bonding materializes from first principles of quantum mechanics in conjunction with the concept

[⊗] Abstract published in *Advance ACS Abstracts,* July 15, 1996.

(1) Mulliken, R. *J. Chem. Phys.* **1955**, *23*, 1833, 2343.
(2) Davidson, E. R. *J. Chem. Phys.* **1967**, *46*, 3320.
(3) Roby, K. R. *Mol. Phys.* **1974**, *27*, 81. Heinzmann, R.; Ahlrichs, R. *Theor. Chim. Acta* **1976**, *33*. Ehrhardt, C.; Ahlrichs, R. *Theor. Chim. Acta* **1985**, *68*, 231.
(4) Reed, A. E.; Weinstock, R. B.; Weinhold, F. *J. Chem. Phys.* **1985**, *83*, 735. Reed, A. E.; Curtiss, L. A.; Weinhold, F. *Chem. Rev.* **1988**, *88*, 899.
(5) Bader, R. F. W. *Atoms in Molecules*; Clarendon Press: Oxford, 1990.
(6) Bader, R. F. W.; Popelier, P. L. A.; Keith, T. A. *Angew. Chem., Int. Ed. Engl.* **1994**, *33*, 620.
(7) See also: Cioslowski, J.; Mixon, S. T. *J. Am. Chem. Soc.* **1991**, *113*, 4142.
(8) Cioslowski, J. *J. Am. Chem. Soc.* **1989**, *111*, 8333.
(9) Becke, A. D.; Edgecombe, K. E. *J. Chem. Phys.* **1990**, *92*, 5397.

of atomic neighborhoods in molecules. At the end of each section we exemplify our approach by some elementary applications.

Section V provides an extensive analysis of the electronic structure of PF_5. This well-known molecule serves as a nontrivial example of how our approach, Sections II−IV, may be applied to elucidate molecular electronic structure. We show that three-center four-electron bonds[10,11] between phosphorus and the axial fluorine atoms are misleading as a description of electronic structure in PF_5, and in this way we contradict older textbook wisdom that is upheld in a recent review.[12]

Standard Computational Techniques. All results reported here have been obtained within the SCF/SVP approximation unless stated otherwise. The acronym SCF/SVP stands for (closed-shell) self-consistent field theory[13,14] (SCF) applied in conjunction with the TURBOMOLE split valence basis set[15] including one shell of polarization functions per atom (SVP).[16] The basis set label TZV2d1f relates to TURBOMOLE triple-ζ valence basis sets[17,18] augmented by polarization functions taken from Dunning's correlation consistent triple-ζ basis sets.[19] Correlation effects have been probed, Section III, by the hybrid density functional B3LYP.[20] All SCF and B3LYP calculations have been performed with the program system TURBOMOLE[21] on workstation computers.

II. Radial Densities and Populations of Atoms in Molecules

Consider the molecular orbitals (MOs) $|i\rangle$ of an SCF wave function or, more generally, natural orbitals[22] of an arbitrary wave function. Without loss of generality we may restrict our consideration to closed-shell systems, that is, we disregard spin. The MOs $|i\rangle$ usually are represented as functions in three-dimensional space:

$$\varphi_i(\underline{r}) = \langle \underline{r}|i\rangle \tag{1}$$

The vector $\underline{r}$ represents a point in three-dimensional space. The continuous set of position eigenfunctions $|\underline{r}\rangle$ forms a complete and orthogonal basis in one-particle space, and one may also write the identity

$$|i\rangle = \int\int\int \mathrm{d}^3\underline{r}\,|\underline{r}\rangle\langle\underline{r}|i\rangle \tag{2}$$

The amplitude $\langle \underline{r}|i\rangle$ of MO $|i\rangle$ at position $\underline{r}$ may be expressed in units of bohr$^{-3/2}$, and the quantity

$$\rho(\underline{r}) = \sum_i \langle \underline{r}|i\rangle n_i \langle i|\underline{r}\rangle = \langle \underline{r}|\hat{D}|\underline{r}\rangle \tag{3}$$

measured in bohr^{-3}, defines the electronic density at position $\underline{r}$. $0 \le n_i \le 2$ is the occupation of MO $|i\rangle$. The one-particle density operator

$$\hat{D} = \sum_i |i\rangle n_i \langle i| \tag{4}$$

has been introduced for later convenience. This is textbook quantum chemistry.[23] It is equally permissible to express MO $|i\rangle$ in terms of a one-center expansion:[24]

$$|i\rangle = \sum_l \sum_m \int_0^\infty \mathrm{d}r\, |A;rlm\rangle\langle A;rlm|i\rangle \tag{5}$$

Here $|A;rlm\rangle$ labels an eigenfunction of radius and of angular momentum (operators $\hat{\underline{l}}^2$ and $\hat{l}_z^2$) with eigenvalues r, $l(l+1)$, and m^2 (in atomic units). m will be given a positive or negative sign, depending on whether $|A;rlm\rangle$ is chosen to behave like cosine or like sine with respect to a reflection at the xz plane. The index A refers to a Cartesian coordinate frame which in chemically relevant applications will be centered at the position of a nucleus. In this way the eigenfunctions $|A;rlm\rangle$ relate to *real* spherical harmonics, centered at nucleus A, and $|A;r,2,-1\rangle$ may also be addressed as $|A;r,d_{yz}\rangle$.

$\langle A;rlm|i\rangle$ will be referred to as an amplitude,[25] expressed in units of bohr$^{-1/2}$, and again

$$\rho_A(r,l,m) = \sum_i \langle A;rlm|i\rangle n_i \langle i|A;rlm\rangle = \langle A;rlm|\hat{D}|A;rlm\rangle \tag{6}$$

defines an electron density: $\rho_A(r,l,m)$ is the number of electrons per bohr having distance r from nucleus A, total angular momentum $l(l+1)$, squared magnetic angular momentum m^2, and symmetric (m positive) or antisymmetric (m negative) properties with respect to reflection at the xz plane.[26]

We further define

$$\rho_A(r,l) = \sum_{|m|\le l} \rho_A(r,l,m) \tag{7}$$

and

$$N_A(R,l) = \int_0^R \mathrm{d}r\, \rho_A(r,l) \tag{8}$$

$N_A(R,l)$ is the average number ("population") of electrons with

(10) Pimentel, G. C. *J. Chem. Phys.* **1951**, *19*, 446.
(11) Rundle, R. E. *J. Am. Chem. Soc.* **1963**, *85*, 112. Rundle, R. E. *Surv. Prog. Chem.* **1963**, *1*, 81.
(12) Gilheany, D. G. *Chem. Rev.* **1994**, *94*, 1339.
(13) Roothaan, C. C. J. *Rev. Mod. Phys.* **1951**, *23*, 69. Hall, G. G. *Proc. R. Soc. London A* **1951**, *205*, 541.
(14) Hehre, W. J.; Radom, L.; Schleyer, P. v. R.; Pople, J. A. *Ab Initio Molecular Orbital Theory*; Wiley-Interscience Publication: New York, 1986.
(15) Schäfer, A.; Horn, H.; Ahlrichs, R. *J. Chem. Phys.* **1992**, *97*, 2571.
(16) Five d functions per d shell are used in all calculations unless indicated otherwise. The *TURBOMOLE* standard polarization function exponents are H 0.8, B 0.5, C 0.8, N 1.0, O 1.2, F 1.4, P 0.45, S 0.55, Cl 0.65, Kr 0.443.
(17) Schäfer, A.; Huber, C.; Ahlrichs, R. *J. Chem. Phys.* **1994**, *100*, 5829.
(18) For phosphorus the basis set labeled TZV' in ref 17 has been employed.
(19) Dunning, T. H. *J. Chem. Phys.* **1989**, *90*, 1007. Woon, D. E.; Dunning, T. H. *J. Chem. Phys.* **1993**, *98*, 1358.
(20) A concise definition of the B3LYP functional is given in: Bauschlicher, C. W.; Partridge, H. *Chem. Phys. Lett.* **1994**, *231*, 277. See also: Becke, A. D. *J. Chem. Phys.* **1993**, *98*, 5648. Becke, A. D. *Phys. Rev. A* **1988**, *38*, 3098. Lee, C.; Yang, W.; Parr, R. G. *Phys. Rev. B* **1988**, *37*, 785. Vosko, S. H.; Wilk, L.; Nusair, M. *Can. J. Phys.* **1980**, *58*, 1200.
(21) Ahlrichs, R.; Bär, M.; Häser, M.; Horn, H.; Kölmel, C. *Chem. Phys. Lett.* **1989**, *162*, 165. Treutler, O.; Ahlrichs, R. *J. Chem. Phys.* **1995**, *102*, 346.
(22) Löwdin, P.-O. *Phys. Rev.* **1955**, *97*, 1474.
(23) An excellent reference is: McWeeny, R. *Methods of Molecular Quantum Mechanics*, 2nd ed.; Academic Press: London, 1992.
(24) Probably the first application of the one-center expansion technique to the calculation of a molecular wave function was by: Finkelstein, B. N.; Horowitz, G. E. *Z. Phys.* **1928**, *48*, 118. For an early bibliography see: Hagstrom, S.; Shull, H. *J. Chem. Phys.* **1959**, *30*, 1314. To the best of our knowledge the one-center expansion technique has never been applied to analyze a general molecular wave function.
(25) The radial amplitudes $\langle A;rlm|i\rangle$ of orbitals of the hydrogen atom are depicted in Figure 5.2.2 of the following: Slater, J. C. *Quantum Theory of Matter*; McGraw-Hill: New York, 1951. Slater refers to the radial amplitudes as r times the radial part of the wave function.
(26) Curves showing the radial density $\rho_A(r,l,m)$ as a function of radius r are well-known for atoms, cf.: Atkins, P. W. *Quanta*; Oxford University Press: Oxford, 1991; p 302 and references therein.

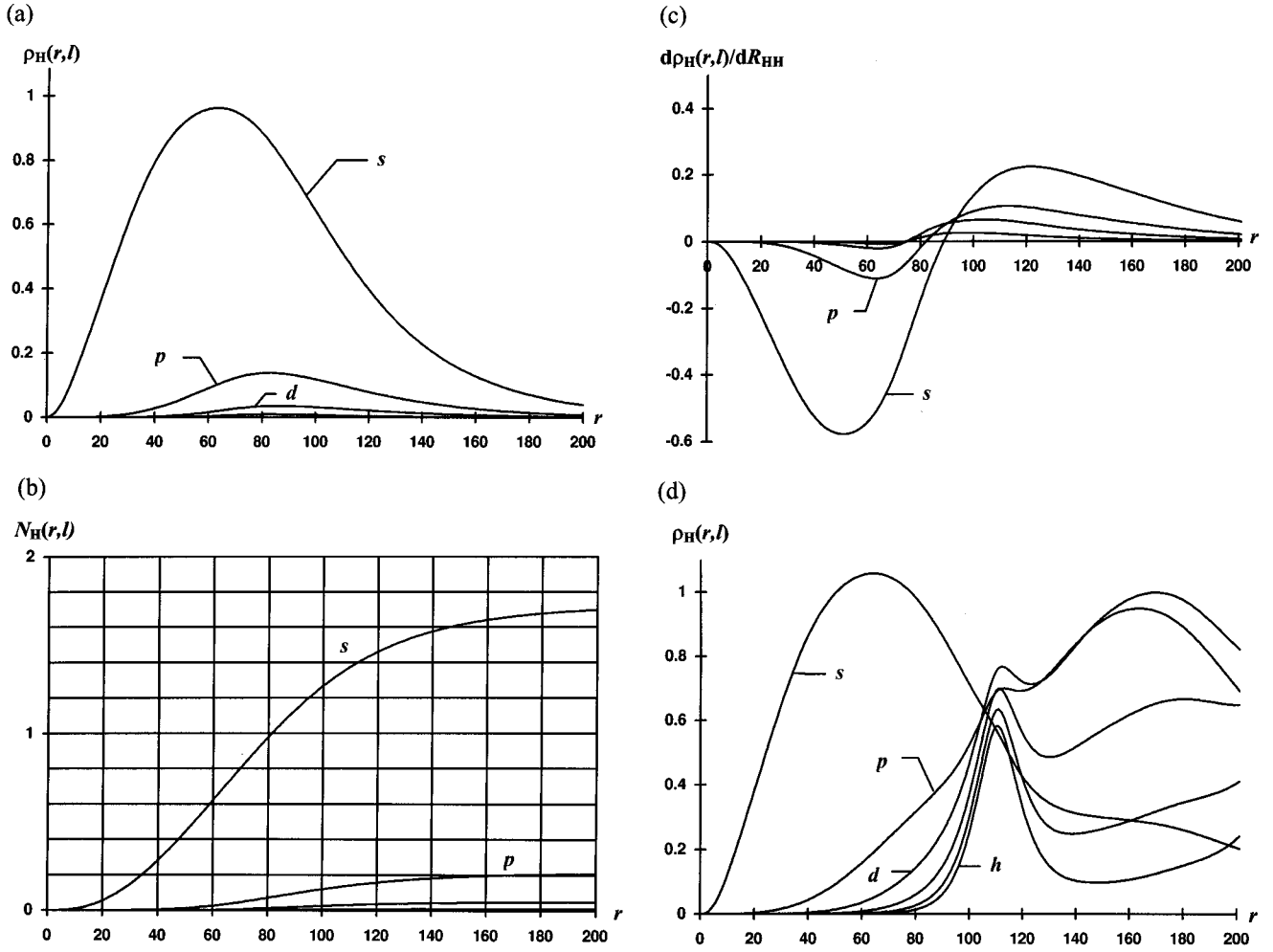

Figure 1. (a) Electronic radial densities $\rho_H(r,l)$ taken with respect to a hydrogen nucleus in H_2 (SCF/SVP approximation; the bond length is 75 pm), given in units of bohr^{-1}, plotted as functions of radius $r < 200$ pm, and labeled by *s*, *p*, *d*, ... according to total angular momentum quantum number $l = 0, 1, 2, ...$ (b) Electronic radial populations $N_H(r,l)$ obtained by integrating $\rho_H(r,l)$, eq 8. (c) Response $d\rho_H(r,l)/dR_{HH}$ (in units of bohr^{-2}) of the radial density $\rho_H(r,l)$ to an increase in the HH bond length R_{HH}. (d) Radial densities $\rho_H(r,l)$ evaluated for a hydrogen atom in ethane (SCF/SVP approximation; the CH bond length is 109 pm).

total angular momentum $l(l + 1)$ within a sphere of radius R around nucleus A. The sum

$$N_A(R) = \sum_l N_A(R,l) \tag{9}$$

is the total electron population within the aforementioned sphere. $N_A(R)$ may also be obtained as the expectation value of the projection operator

$$\hat{P}_A(R) = \sum_l \sum_m \hat{P}_A(R,l,m) = \sum_l \sum_m \int_0^R dr\, |A;rlm\rangle\langle A;rlm| \tag{10}$$

Elementary Applications. We start with H_2. The calculated HH distance is 75 pm. At each nucleus a coordinate system is chosen with the *z* axis pointing at the other nucleus. Figure 1a shows radial densities $\rho_H(r,l) = \rho_H(r,l,0)$ as seen from one of the hydrogen nuclei. The *p* density, i.e., $\rho_H(r,1)$, is at least an order of magnitude smaller than the *s* density. Only near or beyond the distance where the second nucleus resides, $r = 75$ pm, does one notice a small admixture of higher angular momentum densities. This is a consequence of the orbital cusp at the other nucleus, and of the slightly elongated charge cloud of H_2. The radial dependence of the partial populations $N_H(R,l)$, Figure 1b, shows the integrals of the curves from Figure 1a, and confirms the high *s* character of the molecular orbital when seen from any one of the two hydrogen atoms.

Figure 1c displays $d\rho_H(r,l,0)/dR_{HH}$, that is, the response in hydrogen radial densities $\rho_H(r,l,0)$ to a change in the internuclear distance (R_{HH} measured in atomic units). A strong depletion of *s* density in the neighborhood of the hydrogen nucleus can be diagnosed. This response to the stretching of the HH bond is almost an order of magnitude stronger than any responses in the other radial densities (*p*, *d*, ...). The dominant *s* orbital expansion is typical of an *s* orbital taking the greatest share in the covalent bond. There is an additional twist to Figure 1c. First-order properties are generally obtained as first derivatives of the total energy *E* with respect to a corresponding perturbation. Applied to radial densities this means

$$\rho_A(r,l,m) = E^{\lambda} = dE/d\lambda \tag{11}$$

provided $\lambda|A;rlm\rangle\langle A;rlm|$ has been added to the Hamiltonian as a perturbation.[27] Let ξ denote some molecular structure parameter (bond distance, bond angle, ...). Obviously one has

$$d\rho_A(r,l,m)/d\xi = E^{\xi\lambda} = E^{\lambda\xi} \tag{12}$$

In the case of H_2, $A =$ H and $\xi = R_{HH}$. According to eq 12 the curves in Figure 1c thus show the (negative of the) internuclear force (along coordinate ξ) that results when the electronic system

(27) In the many-electron case a sum over operators for each electron has to be written.

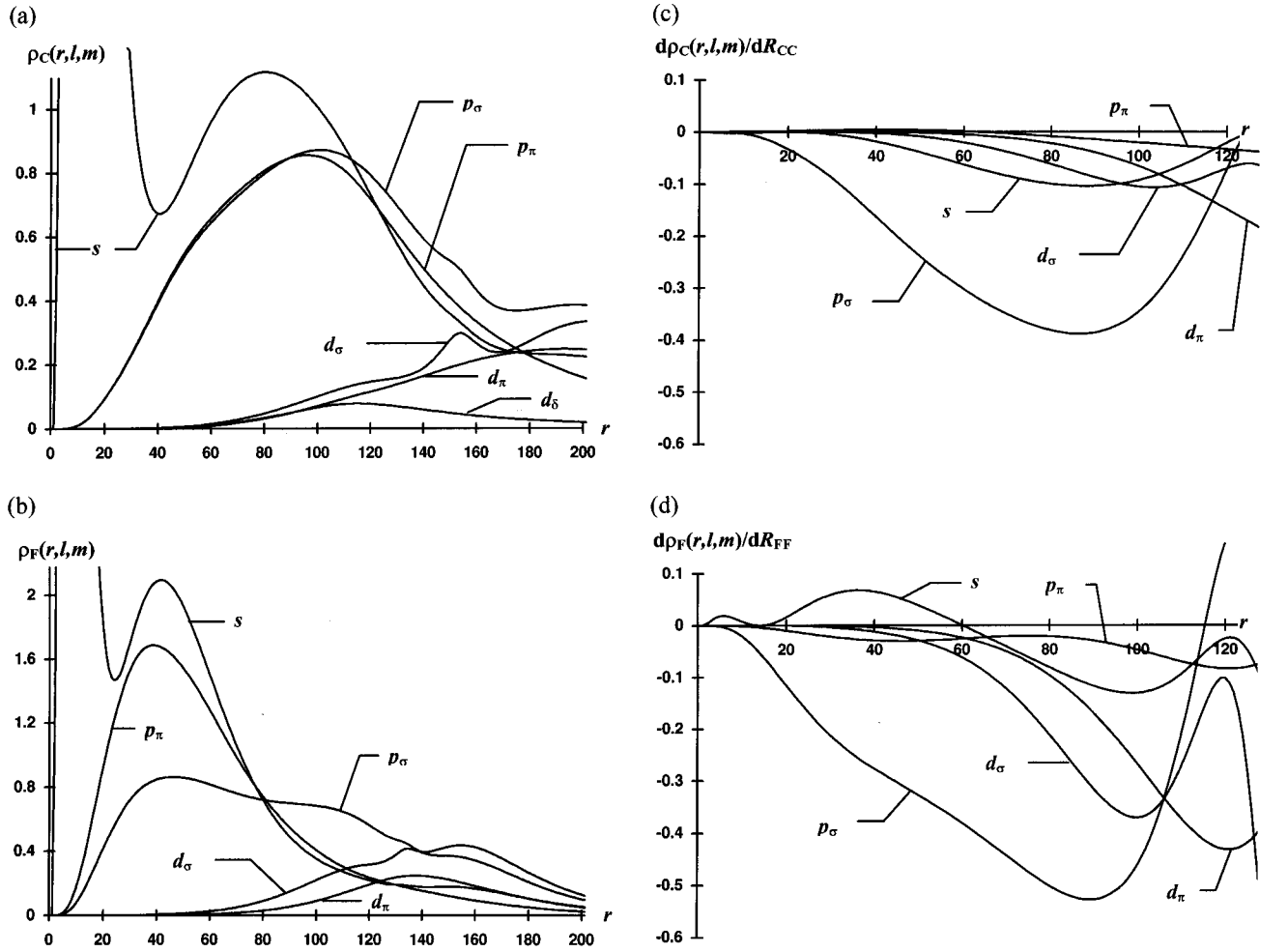

Figure 2. (a) Electronic radial densities $\rho_C(r,l,m)$ for a carbon atom in ethane (SCF/SVP approximation; the bond lengths are $R_{CH} = 109$ pm, $R_{CC} = 153$ pm). The labels *s*, *p*, *d* refer to total angular momentum $l = 0, 1, 2$; σ, π, δ, refer to $|m|$ and mark the symmetry behavior with respect to the CC bond. (b) $\rho_F(r,l,m)$ for a fluorine atom in F_2 (SCF/TZV2d1f approximation; the bond length is 133 pm). (c) Response $d\rho_C(r,l,m)/dR_{CC}$ of the carbon radial density in ethane to a CC bond stretch. (d) $d\rho_F(r,l,m)/dR_{FF}$ in F_2.

is perturbed by $|A;rlm\rangle\langle A;rlm|$, for any choice of r and l and for $m = 0$. For example, if we destabilize *s* electrons at a distance $r \approx 55$ pm from the first hydrogen nucleus in H_2, then Figure 1c tells that a rather strong repulsive force will tend to drive the hydrogen atoms apart.

Figure 1d shows radial densities $\rho_H(r,l)$ of hydrogen in the calculated equilibrium conformation of ethane ($R_{CH} = 109$ pm, $R_{CC} = 153$ pm). Owing to similar bond polarity, the *s* densities in Figure 1a,d can be superimposed onto each other without difference for $r \leq 30$ pm. At larger radii there is slightly more *s* density around H in ethane than in H_2. The (radial) position of the carbon core at 109 pm forms a striking feature, Figure 1d, in the higher angular momentum densities, $\rho_H(r,l)$, $l \geq 1$. This signals outer limits of a meaningful interpretation of $\rho_H(r,l)$.

Figures 2a and 2b depict radial densities, $\rho_A(r,l,m)$, $l \leq 2$, of carbon in ethane, $A = C$, and of fluorine in F_2, $A = F$, respectively. The *z* axis at each non-hydrogen atom is chosen to point toward its corresponding bond partner, and the *x* axes are parallel. One notices the *1s* core electrons of *A* at radii $r <$ 40 pm and the valence densities peaking beyond. At large radii, $r = 140-160$ pm, the cores of the neighboring atoms show up in $\rho_A(r,d_\sigma)$. Hydrogen bond partners indicate their presence by the broad peak in $\rho_C(r,d_\sigma)$, $r \approx 110$ pm. Here we have used the notations d_σ and d_δ for d_{z^2} and d_{xy} (or $d_{x^2-y^2}$), respectively, and will continue to do so in related cases. The much more concentrated valence shell of fluorine as compared to that of carbon is immediately evident from Figures 2a and 2b. However, the fluorine p_σ density is relatively diffuse as it relates to the compararively long FF single bond. Figures 2c and 2d show $d\rho_A(r,l,m)/dR_{AA'}$, $A,A' \in \{C,F\}$, in the ethane and fluorine molecules, respectively. In the case of ethane, the elongation of the CC bond is accompanied by a depopulation of p_σ and—to a lesser degree—*s* density. As was true for H_2, these density responses correspond to an expansion of the *2s* and *2p*$_\sigma$ orbitals which participate in the CC bond. Out-of-phase with these density changes (that is, at 20−30 pm larger radii) one notices also a depletion in d_σ density, but the major contribution to this effect is obviously the other CH_3 fragment dragging its share of the σ bond behind. The case of fluorine, Figure 2d, shows characteristic differences. Here it is only the p_σ density, not the *s* density, which reveals the characteristic orbital expansion upon FF bond stretching. This is in agreement with established knowledge: the FF single bond is composed mainly of the atomic *2p*$_\sigma$ orbitals. The changes in *s* density exhibit the characteristic nodal structure of the *2s* orbital (minimum at 15 pm), and represent contraction of the *2s* orbital. This may be interpreted as a response to the nuclear descreening brought about by the depletion of the p_σ density. The response of p_π densities to a CC (FF) bond stretch is weak in ethane (or F_2) as the corresponding orbitals are not engaged in a covalent bond between these atoms. As a minor effect there is a slight decrease in fluorine p_π densities at small radii upon elongation of the FF bond. For a rationalization imagine that one destabilizes the

p_π orbitals of fluorine at small radii; the response will be an expansion of these orbitals (lone pair expansion); this in turn will increase the repulsive lone pair interaction in F_2; as a consequence $E^{\lambda\xi} < 0$ where ξ is the FF bond distance.

Clearly, $E^{\lambda\xi}$ curves like those in Figures 1c and 2c,d give *indirect* evidence of chemical bonding, but other effects show up, too. A *direct* probe for covalence will be introduced in Section IV.

III. Characterization of Atomic Valence in Molecules

Atomic Neighborhood Natural Orbitals (ANNO). To obtain a more detailed picture of the electronic environment in which atom *A* is embedded we strive to represent the electronic one-particle density in a neighborhood of *A* by as few orbitals[28] $|A,R;\tilde{\alpha}\rangle$ as possible. That is, for arbitrary radius *R*, we choose *M* orthonormal orbitals $|A,R;\tilde{\alpha}\rangle$, $\alpha = 1, 2, ..., M$, for which the projector

$$\hat{P}_A(M,R) = \sum_{\alpha=1}^{M} |A,R;\tilde{\alpha}\rangle\langle A,R;\tilde{\alpha}| \qquad (13)$$

has the properties

$$\hat{P}_A(M,R) = \hat{P}_A(M,R)\hat{P}_A(R) = \hat{P}_A(R)\hat{P}_A(M,R) \qquad (14)$$

and

$$\text{trace}(\hat{D}\hat{P}_A(M,R)) = \text{maximum} \qquad (15)$$

For $R \rightarrow \infty$ the natural orbitals[22] are recovered. For arbitrary radius *R* the orbitals $|A,R;\tilde{\alpha}\rangle$ are a straightforward generalization of natural orbitals—in fact they are natural orbitals in a spherical neighborhood of *A*—and they will henceforth be called atomic neighborhood natural orbitals (ANNO). They are solutions to the eigenvalue equations

$$\hat{P}_A(R)\hat{D}\hat{P}_A(R)|A,R;\tilde{\alpha}\rangle = |A,R;\tilde{\alpha}\rangle n_\alpha(A,R) \qquad (16)$$

The eigenvalues $0 \le n_\alpha(A,R) \le 2$ are the occupancies of the ANNOs $|A,R;\tilde{\alpha}\rangle$. Computationally it is more convenient to consider the equivalent eigenvalue problem[29]

$$\hat{D}^{1/2}\hat{P}_A(R)\hat{D}^{1/2}|A,R;\alpha\rangle = |A,R;\alpha\rangle n_\alpha(A,R) \qquad (17)$$

which is obtained from eq 16 upon the substitution

$$|A,R;\alpha\rangle = n_\alpha(A,R)^{-1/2}\hat{D}^{1/2}\hat{P}_A(R)|A,R;\tilde{\alpha}\rangle \qquad (18)$$

With respect to closed-shell SCF wave functions the orbitals $|A,R;\alpha\rangle$ with largest occupations $n_\alpha(A,R)$ are best-localized in a neighborhood of *A* with radius *R*. Thus $|A,R;\alpha\rangle$ would best be denoted as an atomic neighborhood localized orbital (ANLO). It is often inconvenient to use different acronyms for entities that are largely equivalent. Therefore one may use the acronym ANNO for both $|A,R;\tilde{\alpha}\rangle$ and $|A,R;\alpha\rangle$, unless a distinction is really necessary.

We will characterize ANNOs by how much *s*, p_x, d_{xy}, ..., etc. population they contribute in a neighborhood of *A*, that is, we evaluate

$$n_\alpha(A,R,l,m) = \langle A,R;\alpha|\hat{D}^{1/2}\hat{P}_A(R,l,m)\hat{D}^{1/2}|A,R;\alpha\rangle = n_\alpha(A,R)\langle A,R;\tilde{\alpha}|\hat{P}_A(R,l,m)|A,R;\tilde{\alpha}\rangle \qquad (19)$$

It is important to understand that $n_\alpha(A,R,l,m)$ as a continuous function of $R \in (0;\infty)$ characterizes a continuous set of orbitals $|A,R;\tilde{\alpha}\rangle$ or $|A,R;\alpha\rangle$. This continuous set of orbitals is referred to by the label α. The reader should be aware that we will use the acronym ANNO when we refer to individual orbitals $|A,R;\alpha\rangle$, that is, *R* is fixed, and when we adress a whole class of orbitals $|A,R;\alpha\rangle$, $R \in (0;\infty)$.

The ANNO approach is rigorously built on first principles of quantum mechanics, the mathematical definition of a spherical neighborhood, the definition of angular momentum eigenfunctions, and the one-particle density to be scrutinized. What comes out of it are *functions* of radius like $n_\alpha(A,R,l,m)$ that characterize the molecular electronic structure from an atomic point of view or, in other words, that characterize the one-particle density operator in any spherical neighborhood of *A*. These *functions* may serve as a first-principles basis of a comparison between "atoms" in molecules.

Pictorial Interpretation of ANNOs. Hypervalence. Visualize a small spherical neighborhood of radius *R* around nucleus *A*. Imagine that as you scan through larger and larger radii *R* you sample an increasing fraction of the electronic environment surrounding nucleus *A*. At *each* radius *R* you ask: How many orbitals are necessary to represent the one-particle density inside that neighborhood of *A*, what is the error of that approximation, and what are the properties of these orbitals? Clearly these questions relate to the role of (hyper-) valence at *A*.[30]

The above-posed problem can be adressed by utilizing the orbitals $|A,R;\tilde{\alpha}\rangle$ or $|A,R;\alpha\rangle$ (ANNOs).[31] They are characterized by their composition $n_\alpha(A,R,l,m)$ and occupation $n_\alpha(A,R) = \sum_{l,m} n_\alpha(A,R,l,m)$ *inside* any spherical neighborhood of *A* with radius *R*. Abberations from, e.g., the octet rule simply relate to the difference

$$\Delta N_A(M,R) = N_A(R) - \sum_{\alpha=1}^{M} n_\alpha(A,R) \qquad (20)$$

between the total electronic population at *A* and the electronic population that is representable in terms of *M* orbitals. To test the octet rule, *M* would have to be chosen equal to the number of core and valence atomic orbitals of the isolated atom *A*.

For isolated atoms *A* the derivative of the function $n_\alpha(A,R)$ is closely related but usually not identical to radial distribution functions of individual spectroscopic orbitals.[32,33]

Labeling of ANNOs. The ANNOs $|A,R;\alpha\rangle$ often display nodal characteristics of atomic orbitals. We use the labels $\alpha =$ *1s, 2s, ..., 3p$_z$, 3d$_{xy}$, ...* correspondingly. For example, if an

(28) An orbital is an occupied one-electron state function. Orbitals in a rigorous sense exist only in one-electron systems or if electronic correlation is neglected. Spectroscopic orbitals characterize some major *difference* between initial and final many-electron states—a difference that can approximately be expressed within a one-particle picture. The one-particle density of a *single* many-electron state can best be approximated by a limited number of partially occupied orbitals, *if* natural orbitals[22] are considered. In the following text we build upon the natural orbital concept as opposed to the spectroscopic orbital concept.

(29) The equivalence is restricted to non-zero eigenvalues $n_\alpha(A,R)$.

(30) An atom of a main group element may be said to be engaged in hypervalent interactions, if the octet rule is violated. The octet rule is violated if a corresponding number of orbitals does not provide a qualitatively satisfactory description of the molecular electronic structure surrounding the nucleus. To quantify the importance of hypervalent interactions, it is necessary to consider their energetic effects, too. First steps in that direction are taken in a later discussion of bonding in PF_5.

(31) For closed-shell SCF wave functions the amplitudes of ANNOs $|A,R;\tilde{\alpha}\rangle$ and of ANLOs $|A,R;\alpha\rangle$ are proportional to each other inside a sphere of radius *R* centered at *A*. Outside that atomic neighborhood the amplitude of ANNOs is zero while that of ANLOs is continuous.

(32) For the H atom $dn_\alpha(H,R)/dR$ corresponds to the quantity depicted in Figure 21-3 of the following: Pauling, L.; Wilson, E. B. *Introduction to Quantum Mechanics*; McGraw-Hill: New York, 1935.

Table 1. Atomic Neighborhood Natural Orbitals (ANNOs) $|C,R;\alpha\rangle$ of Carbon in Staggered Ethane (SCF/SVP)[a]

α	*l*,*m*[b]	10	20	30	40	50	60	70	80	90	100
1s	*s*	0.7355	1.6059	1.9091	1.9824	1.9972	1.9995	1.9998	1.9999	1.9999	1.9999
2s	*s*	0.0000	0.0000	0.0000	0.0115	0.2240	0.3916	0.5880	0.7971	1.0052	1.2013
	p_z	0.0005	0.0104	0.0427	0.0934	0.0004	0.0000	0.0000	0.0002	0.0006	0.0010
	3,−3	0.0000	0.0000	0.0000	0.0000	0.0000	0.0001	0.0003	0.0011	0.0025	0.0049
	3,0	0.0000	0.0000	0.0000	0.0000	0.0000	0.0001	0.0004	0.0013	0.0030	0.0061
$2p_z$	*s*	0.0001	0.0049	0.0317	0.0907	0.0003	0.0000	0.0000	0.0001	0.0005	0.0008
	p_z	0.0000	0.0000	0.0000	0.0111	0.1957	0.3109	0.4428	0.5886	0.7452	0.9081
	d_{z^2}	0.0000	0.0000	0.0000	0.0000	0.0010	0.0029	0.0069	0.0140	0.0252	0.0413
	3,−3	0.0000	0.0000	0.0000	0.0000	0.0000	0.0000	0.0001	0.0004	0.0011	0.0022
	3,0	0.0000	0.0000	0.0000	0.0000	0.0000	0.0000	0.0000	0.0002	0.0006	0.0014
$2p_y$	p_y	0.0005	0.0104	0.0431	0.1059	0.1992	0.3164	0.4510	0.5992	0.7570	0.9181
	d_{yz}	0.0000	0.0000	0.0000	0.0001	0.0004	0.0012	0.0029	0.0060	0.0107	0.0174
	d_{xy}	0.0000	0.0000	0.0000	0.0001	0.0007	0.0020	0.0049	0.0099	0.0177	0.0285
	3,2	0.0000	0.0000	0.0000	0.0000	0.0000	0.0000	0.0002	0.0007	0.0018	0.0036
$3d_{yz}$	p_y	0.0000	0.0000	0.0000	0.0000	0.0000	0.0000	0.0000	0.0001	0.0003	0.0007
	d_{yz}	0.0000	0.0000	0.0000	0.0000	0.0002	0.0006	0.0014	0.0031	0.0060	0.0108
	d_{xy}	0.0000	0.0000	0.0000	0.0000	0.0000	0.0000	0.0000	0.0002	0.0003	0.0006
	3,−1	0.0000	0.0000	0.0000	0.0000	0.0000	0.0000	0.0001	0.0003	0.0011	0.0026
$3d_{z^2}$	*s*	0.0000	0.0000	0.0000	0.0000	0.0000	0.0000	0.0000	0.0001	0.0002	0.0006
	p_z	0.0000	0.0000	0.0000	0.0000	0.0000	0.0000	0.0000	0.0001	0.0004	0.0010
	d_{z^2}	0.0000	0.0000	0.0000	0.0000	0.0000	0.0000	0.0002	0.0004	0.0007	0.0012
	3,0	0.0000	0.0000	0.0000	0.0000	0.0000	0.0000	0.0000	0.0000	0.0000	0.0001

[a] Each ANNO is characterized by its partial populations $n_\alpha(C,R,l,m)$, eq 19, for $R = 10, 20, ..., 100$ pm (numbers are truncated after four postdecimal digits). Symmetry-redundant orbitals have been omitted. The bond distances are $R_{CH} = 109$ pm and $R_{CC} = 153$ pm. [b] Carbon atoms are on the *z* axis.

ANNO $|A,R;\alpha\rangle$ has no radial nodes for a reasonable choice of *R*, and if $n_\alpha(A,R,d_{xy}) \approx n_\alpha(A,R)$, then we refer to it as $|A,R,3d_{xy}\rangle$. This is not a matter of principle, but merely a notation.

Elementary Applications. Figure 1b shows the populations $N_H(R,l) = N_H(R,l,0)$ for the hydrogen atom in H_2 as a function of radius *R* and angular momentum *l*. In this simple case only one MO exists, and thus $N_H(R,l,m) = n_\alpha(H,R,l,m)$ where α labels the only existing ANNO. Since $n_\alpha(H,R) \approx n_\alpha(H,R,0,0) = n_\alpha(H,R,s)$, we may speak of an *s*-type ANNO of hydrogen. If we were to probe its nodal characteristics, cf. Figure 1a, we would find that the notation $\alpha = 1s$ were appropriate.

As a second example consider ANNOs of carbon in ethane, Table 1. Coordinate frames are fixed to the carbon atoms so that the *z* axes point at each other, and *x* axes are parallel. Then the ANNO labeled $2p_y$ is symmetry equivalent to a $2p_x$ ANNO. Only the former is included in Table 1. Its composition up to $R = 100$ pm is almost entirely of p_y character, with very minor contaminations from *d* and *f* functions. Contributions from even higher angular momentum functions are exceedingly small, and are not shown in Table 1. The hypervalent ANNO labeled $3d_{yz}$ (and its symmetry-equivalent partner $3d_{xz}$) is rather weakly occupied, and relates to the CH bonds at the other carbon atom. The well-known result that the electronic structure surrounding a carbon atom in ethane is well-represented by five orbitals is immediately evident from Table 1.

We address two chemically less relevant features in Table 1 that will endow us with a deeper understanding of the ANNO approach. The ANNO labeled *1s* represents the spectroscopic core orbital of carbon, provided *R* is chosen sufficiently large. For smaller radii, $R \leq 40$ pm, the *1s* ANNO is a superposition of the spectroscopic *1s* orbital with a valence *s* orbital so that the density within radius *R* is maximized. As a consequence the one-particle density in the immediate neighborhood of the carbon nucleus, $R \leq 20$ pm, is well-represented by only one orbital. The second point we wish to mention is an "avoided crossing" between the *2s* ANNO and the $2p_z$ ANNO near $R = 41$ pm. The second-most populated σ-type ANNO, i.e. the one that bears the label *2s*, is a continuous set of orbitals of p_z type for $R \leq 40$ pm, and of *s* type at larger radii. If one is interested only in hypervalence at carbon one may dispose of such less relevant information by just comparing the total electronic population, here $N_C(R)$, to its hypervalent share, here $\Delta N_C(5,R)$, eq 20.

In Section V phosphorus ANNOs in PF_3 and PF_5 will be studied.

IV. Covalence and Delocalization: Electron Sharing[34]

It is well-known that the density matrix $D(\underline{r},\underline{r}')$ in configuration space, defined through

$$\hat{D} = \int\int\int \mathrm{d}^3\underline{r} \int\int\int \mathrm{d}^3\underline{r}' \, |\underline{r}\rangle D(\underline{r},\underline{r}')\langle\underline{r}'| \qquad (21)$$

provides a measure of delocalization. For example, in extended crystalline systems with completely filled bands $|D(\underline{r},\underline{r}')|$ decreases exponentially as $|\underline{r} - \underline{r}'| \rightarrow \infty$.[35] In metals $|D(\underline{r},\underline{r}')|$ decreases only like an inverse power in $|\underline{r} - \underline{r}'|$.[36] Unfortunately, $D(\underline{r},\underline{r}')$ is a six-dimensional field, and inconvenient for

(33) In many-electron atoms there is no *a priori* unique way to separate, e.g., *1s* and *2s* orbitals. Any such distinction refers to a particular type of measurement. Here we subject the atomic electronic structure to the continuous set of projection operators, $\hat{P}_A(R)$, $R \in (0;\infty)$. Each choice of *R* will in general recover slightly different "natural" *1s* and *2s* orbitals. Thus, while for each choice of *R* the occupation $n_\alpha(A,R)$ refers to a single orbital $|A,R;\tilde{\alpha}\rangle$, the function $n_\alpha(A,R)$, $R \in (0;\infty)$, refers to a continuous set of orbitals $|A,R;\tilde{\alpha}\rangle$, $R \in (0;\infty)$. The same holds in molecules, except that now even the distinction between, e.g. *s*- and *p*-type orbitals will be lost.

(34) In case of an SCF wave function an electron may be said to be shared between two one-particle state functions $|a\rangle$ and $|b\rangle$, if and only if in *each* orbital representation of the many-electron wave function at least one orbital $|i\rangle$ has non-zero overlap with both $|a\rangle$ and $|b\rangle$. It may be shown that this condition is equivalent to the existence of an orbital representation for the SCF wave function in which one and only one orbital $|i\rangle$ has non-zero overlap with $|a\rangle$ and $|b\rangle$, and that it is also equivalent to the one-electron operator $^1/_2(|a\rangle\langle b| + |b\rangle\langle a|)$ having a non-zero expectation value. The latter expectation value may serve as a straightforward quantification of electron sharing between $|a\rangle$ and $|b\rangle$ in the case of general (real) wave functions. The expectation value of $^1/_2(|a\rangle\langle b| + |b\rangle\langle a|)$ may also be said to measure one-electron coherence or delocalization between $|a\rangle$ and $|b\rangle$. Traditionally, the term electron sharing is often applied, if $|a\rangle$ and $|b\rangle$ are atomic functions that participate in a covalent bond. Delocalization, on the other hand, relates to electron sharing phenomena among atomic functions that in part are well separated. Here we use electron sharing (or electronic coherence) as a general term, and covalence and delocalization in a more restricted sense.

(35) de Cloizeaux, J. *Phys. Rev. A* **1964**, *135*, 685.

(36) Monkhorst, H. J.; Kertesz, M. *Phys. Rev. B* **1981**, *24*, 3015.

direct analysis of molecular electronic structure. Instead we propose to consider molecular delocalization phenomena on the basis of the one-center expansion technique:

$$\hat{D} = \sum_{l_A l_B m_A m_B} \int_0^\infty dr_A \int_0^\infty dr_B \, |A;r_A l_A m_A\rangle \omega_{AB}(r_A,l_A,m_A;r_B,l_B,m_B) \langle B;r_B l_B m_B| \quad (22)$$

where the density matrix

$$\omega_{AB}(r_A,l_A,m_A;r_B,l_B,m_B) = \sum_i \langle A;r_A l_A m_A|i\rangle n_i \langle i|B;r_B l_B m_B\rangle \quad (23)$$

makes reference to two possibly different centers (atoms) *A* and *B*.

ω_{AB} may alternatively be obtained as an expectation value of the Hermitian operator

$$\hat{O}_{AB}(r_A,l_A,m_A;r_B,l_B,m_B) = {}^1/_2(|A;r_A l_A m_A\rangle\langle B;r_B l_B m_B| + |B;r_B l_B m_B\rangle\langle A;r_A l_A m_A|) \quad (24)$$

through

$$\omega_{AB}(r_A,l_A,m_A;r_B,l_B,m_B) = \text{trace } \hat{D}\,\hat{O}_{AB}(r_A,l_A,m_A;r_B,l_B,m_B) \quad (25)$$

The two definitions, eqs 23 and 25, appear identical, provided the MOs (or natural orbitals) are real or can be brought to real form.[37] Comparison to eq 6 reveals

$$\omega_{AA}(r_A,l_A,m_A;r_A,l_A,m_A) = \rho_A(r_A,l_A,m_A) \quad (26)$$

In general, ω_{AB} will not be a density as it may be negative. Equations 24 and 25 tell us that, for example, $\omega_{AB}(r_A,d_{xz};r_B,p_x)$ is the average product of amplitudes for the one-electron states $|A;r_A,d_{xz}\rangle$ and $|B;r_B,p_x\rangle$. In other words, $\omega_{AB}(r_A,d_{xz};r_B,p_x)$ measures to which extent one-electron states like d_{xz} at atom *A* and p_x at atom *B* are populated *in phase* (share electrons[34]) as a function of two radii, r_A and r_B, that refer to the nuclei *A* and *B*, respectively. A function like $\omega_{AB}(r_A,d_{xz};r_B,p_x)$ will be addressed as a (d_π−p_π) electron sharing function of *A* and *B* (in the example the *z* axis runs from *A* to *B*).

Electron sharing is a *necessary* ingredient of covalent bonding. On the other hand, electron sharing (or one-electron coherence) as quantified by eq 25 is not exclusively restricted to covalent bond partners, but is characteristic of electron delocalization phenomena of all kinds.[34]

Consistent with that insight, it is not easy to assign attributes like "bonding" or "antibonding" to features of an electron sharing function like $\omega_{AB}(r_A,d_{xz};r_B,p_x)$. This is not so much a problem of our definition as it is a consequence of the potential complexity of electron delocalization phenomena. If attributes like "bonding" or "antibonding" apply at all, one expects to be able to distinguish between these two possibilities using the sign of $\omega_{AB}(r_A,d_{xz};r_B,p_x)$. This sign depends on the coordinate systems (and more generally phase conventions) chosen upon construction of the operator $\hat{O}_{AB}$. Unless mentioned otherwise, we choose the coordinate systems at the nuclei *A* and *B* so that the *z* axes point at each other, while the *x* axes (and the *y* axes) are parallel. p_σ functions centered at *A* and *B* respectively then have lobes of positive sign pointing at each other. p_σ−p_σ electron sharing would then be qualified as "bonding" *in terms of a Hückel model*, if $\omega_{AB}(r_A,p_z;r_B,p_z)$ has a positive sign (for reasonable choices of r_A, r_B). A more rigorous approach is possible: if we amplify electron sharing specifically by forcing a corresponding constraint upon the electronic wave function, we may find (upon subsequent relaxation of the molecular structure) a shortening of the *AB* distance (which would indicate "bonding" electron sharing), or we might find the contrary or some other response of the molecular structure characteristic of the type of delocalization phenomenon affected. We plan to report about the application of such techniques in another contribution.

Elementary Applications. For the hydrogen molecule treated in the SCF approximation

$$\omega_{AB}(r_A,l_A,m_A;r_B,l_B,m_B) = \omega_{AA}(r_A,l_A,m_A;r_B,l_B,m_B) \quad (27)$$

and using eq 26,

$$\omega_{AB}(r,l,m;r,l,m) = \rho_A(r,l,m) \quad (28)$$

Figure 1a thus depicts the electron sharing function(s) $\omega_{AB}(r,l,m;r,l,m)$ of the hydrogen atoms in H_2. In the immediate neighborhood of each hydrogen nucleus, $r \leq 30$ pm, one notices *1s*-type waves sharing their electrons. Figure 1c shows $d\omega_{AB}(r,l,m;r,l,m)/dR_{AB}$. Without proof we mention that if electronic correlation is properly accounted for in H_2, then eqs 27 and 28 will no longer hold. In that case $\omega_{AB} \equiv 0$ in the limit of an infinite nuclear distance (electron sharing is given up in favor of left−right correlation, i.e., two isolated hydrogen atoms form) even though in the restricted Hartree−Fock (SCF) approximation one still has $\omega_{AB}(r,l,m;r,l,m) = \rho_A \neq 0$.

Equation 28 is a special case of

$$|\omega_{AB}(r_A,l_A,m_A;r_B,l_B,m_B)| \leq \rho_A(r_A,l_A,m_A)^{1/2}\rho_B(r_B,l_B,m_B)^{1/2} \quad (29)$$

This inequality is a consequence of $\hat{D}$ having only non-negative eigenvalues.

Delocalization in fluorine (F_2) is analyzed in Figure 3a. The curve labeled p_σ−p_σ refers to the p_σ−p_σ electron sharing function $\omega_{FF'}(r,p_\sigma;r,p_\sigma)$ of the two fluorine atoms F and F′. $\omega_{FF'}(r,p_\sigma;r,p_\sigma)$ is largest where $\rho_F(r,p_\sigma)$ peaks, cf. Figure 2b, at and slightly beyond $r = 40$ pm. If the different scales of the drawings, Figures 2b and 3a, are taken into account, one will notice that $\rho_F(r,p_\sigma) \approx \omega_{FF'}(r,p_\sigma;r,p_\sigma)$, corresponding to "perfect" p_σ−p_σ electron sharing between F and F′, at least for $r \leq 50$ pm. s−p_σ electron sharing becomes significant only for larger radii *r*. If we imagine a pair of electron sharing hybrid orbitals in F_2, then each hybrid orbital—to be consistent with the electron sharing functions—will display almost pure p_σ character at small radii, $r \leq 40$ pm, whereas at larger radii some *s* character will be mixed in (improving directionality).

s−s electron sharing in F_2 is (Hückel) antibonding at small radii, Figure 3a, and may be said to be nonbonding in total. It is remarkable that $\omega_{FF'}(r,s;r,s)$, Figure 3a, shows the same qualitative behavior as $-d\rho_F(r,s)/dR_{FF'}$, Figure 2d. In Section II this behavior has been attributed to a contraction of the *s* orbital upon bond-breaking, in part caused by a descreening of the fluorine nucleus. Figure 3a offers an additional or alternative explanation: the valence *s* orbital contracts upon bond-breaking, because its outer fringes are no longer needed for σ bonding. Admittedly, every reader should be suspicious when it comes to "because": any rigorous analysis of an electronic wave

(37) Otherwise only the real part of ω_{AB} will be recovered by $\hat{O}_{AB}$; the imaginary part is the expectation value of the Hermitian operator $Q_{AB} = (1/2i)(|A;r_A l_A m_A\rangle\langle B;r_B l_B m_B| - |B;r_B l_B m_B\rangle\langle A;r_A l_A m_A|)$. Additional complications arise, if a (magnetic) gauge field is added to the Hamiltonian. In that case the *phase* of off-diagonal density matrix elements like $D(r,r')$ may adopt any value, and in this way is revealed to be non-observable. However, the problem is alleviated by introducing the correct gauge-dependencies into the non-local operators $\hat{O}_{AB}$ and Q_{AB}, and by using these gauge-dependent operators to evaluate ω_{AB} as the expectation value. We will not track the subject of non-real wave functions further.

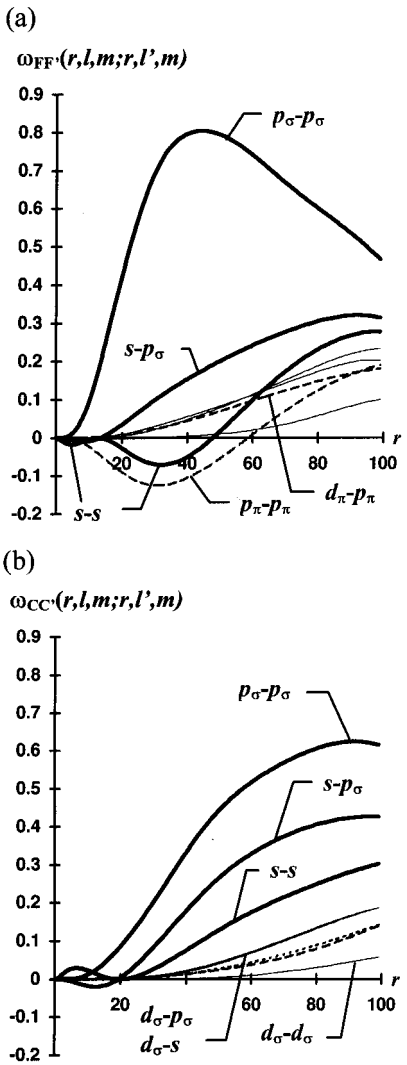

Figure 3. Electron sharing between one-electron states $|A;r,l,m\rangle$ and $|B;r,l',m\rangle$ at atoms *A* and *B*, expressed by the electron sharing functions $\omega_{AB}(r,l,m;r,l',m)$, eqs 24 and 25. The curve labeled $s-p_\sigma$, for example, refers to $\omega_{AB}(r,s;r,p_\sigma)$ plotted as a function of *r*. (a) *A* and *B* are two fluorine atoms in F_2 (SCF/TZV2d1f). (b) *A* and *B* are two carbon atoms in ethane (SCF/SVP). Dashed curves refer to π interactions.

function will at best reveal *facts* (like Figures 1−3) whereas *causes* are harder to come by (they more or less depend on some additional context).

Figure 3a furthermore indicates minor $p_\pi-p_\pi$ electron sharing of Hückel antibonding character. For a rationalization recall that π-type lone pairs of F_2 may form bonding and antibonding linear combinations (in terms of Hückel theory), and the antibonding combination will have larger amplitudes in the vicinity of the nuclei.

When we apply a similar analysis to the carbon atoms in ethane, Figure 3b, we observe significant $p_\sigma-p_\sigma$, $s-p_\sigma$, and $s-s$ electron sharing. The relative weights of these phenomena almost exactly correspond to two sp_σ^3 hybrids engaged in a covalent bond, 40 pm $\le r \le$ 70 pm. While it is not immediately obvious from Figure 3b we note that complementary $s^3(-p_\sigma)$ hybrids would show little electron sharing. Unlike in F_2, $p_\pi-p_\pi$ electron sharing in ethane is weakly (Hückel) bonding. This delocalization effect may be attributed to the engagement of the carbon p_π orbitals in the CH bonds. The effect is slightly stronger in staggered ethane than in the eclipsed conformation (not shown), but it is not the source of the torsion barrier: if the degree of $p_\pi-p_\pi$ electron sharing in staggered ethane is constrained to that in eclipsed ethane, the energy rises by only of the order of 1 kJ/mol, which is one order of magnitude less than the torsion barrier.

This example demonstrates the evaluation of energies that relate to changes in electron sharing properties. Similarly we could require that $p_\sigma-p_\sigma$ electron sharing at $r = 40$ pm in F_2 be weak at the equilibrium distance, e.g., $\omega_{FF'}(r,p_\sigma;r,p_\sigma) = 0.2$, compare Figure 3a. This would probe the *energetic* importance of electron sharing in F_2. However, since we have not yet adapted our program for an application to correlated wave functions, a meaningful study of covalent bond breaking (at the equilibrium bond distance) is not feasible at present.

For similar reasons it will not be investigated here how much energy is necessary to destroy delocalization in benzene, but we will nevertheless close our elementary applications by considering electron sharing *per se* in this prototypical aromatic molecule. As customary we denote by p_π the *p*-type functions perpendicular to the molecular plane, and look at the $p_\pi-p_\pi$ electron sharing function $\omega_{AB}(r_A,p_\pi;r_B,p_\pi)$ of two carbon atoms *A*, *B*. For our intentions it is sufficient to restrict such analysis to the maxima of $|\omega_{AB}(r_A,p_\pi;r_B,p_\pi)|$ which occur at radii $r_{max}(A,B) = r_A = r_B$. For an SCF/SVP wave function one finds $\Omega_{AB} = \omega_{AB}(r_{max}(A,B),p_\pi;r_{max}(A,B),p_\pi) = 0.58$ when $A = B$, $\Omega_{1,2} = 0.40$, $\Omega_{1,3} = -0.01$, and $\Omega_{1,4} = -0.17$.[38,39] Numbers obtained within a simple Hückel model would be very similar. Obviously there is no electron sharing between p_π functions that belong to carbon atoms in *meta* positions ($\Omega_{1,3}$). Delocalization of the π system in benzene is testified by electron sharing between p_π functions in *para* positions ($\Omega_{1,4}$). These results imply that any perturbation applied to a p_π orbital at one carbon atom will coherently affect also the p_π orbital in the *para* position while a p_π orbital in the *meta* position can be influenced only indirectly; this rationalizes substituent effects in electrophilic substitutions. Population analyses (which utilize "overlap" rather than the operator $\hat{O}_{AB}$) have difficulties in revealing *para* $p_\pi-p_\pi$ electron sharing, since the overlap between 1,4-positions is marginal.

Pairs of Electron Sharing Atomic Neighborhood Orbitals. As previously indicated for the example of σ bonding in ethane and F_2, electron sharing between two one-electron states like $|A;r_A l_A m_A\rangle$ and $|B;r_B l_B m_B\rangle$ may appear more pronounced, if hybrid states (superpositions of real spherical harmonics) are considered at each atom. In general one may search for *M* orthonormal orbitals $|A,R_A;\tilde{h}\rangle$, and for the same number of orthonormal orbitals $|B,R_B;\tilde{h}\rangle$, subject to the following conditions:

$$\sum_{h\le M} |A,R_A;\tilde{h}\rangle\langle A,R_A;\tilde{h}| = \hat{P}_A(R_A)\sum_{h\le M} |A,R_A;\tilde{h}\rangle\langle A,R_A;\tilde{h}| = \sum_{h\le M} |A,R_A;\tilde{h}\rangle\langle A,R_A;\tilde{h}|\hat{P}_A(R_A) \quad (30)$$

$$\sum_{h\le M} |B,R_B;\tilde{h}\rangle\langle B,R_B;\tilde{h}| = \hat{P}_B(R_B)\sum_{h\le M} |B,R_B;\tilde{h}\rangle\langle B,R_B;\tilde{h}| = \sum_{h\le M} |B,R_B;\tilde{h}\rangle\langle B,R_B;\tilde{h}|\hat{P}_B(R_B) \quad (31)$$

and

$$\mathrm{trace}(\hat{D}\hat{O}_{AB}(M,R_A,R_B)) = \mathrm{maximum} \quad (32)$$

(38) The radii $r_{max}(A,B)$ are 98, 103, 45, and 74 pm, respectively.
(39) The carbon atoms are numbered from 1 to 6 according to IUPAC conventions.

where

$$\hat{O}_{AB}(M,R_A,R_B) = {}^1/_2 \sum_{h \le M} (|A,R_A;\tilde{h}\rangle\langle B,R_B;\tilde{h}| + |B,R_B;\tilde{h}\rangle\langle A,R_A;\tilde{h}|) \quad (33)$$

$|A,R_A;\tilde{h}\rangle$ and $|B,R_B;\tilde{h}\rangle$ thus represent a pair of hybrid orbitals that are restricted to the atomic neighborhoods characterized by the nuclei *A*, *B* and by the radii R_A and R_B, respectively. These hybrid orbitals are required to maximize their mutual electron sharing properties, eq 32. Such a *p*air of *e*lectron *s*haring *h*ybrid *o*rbitals will be called PESHO. PESHOs may be obtained by solving the eigenvector equations

$$\hat{P}_A(R_A)\hat{D}\hat{P}_B(R_B)\hat{D}\hat{P}_A(R_A)|A,R_A;\tilde{h}\rangle = |A,R_A;\tilde{h}\rangle\eta_h(A,R_A;B,R_B)^2 \quad (34)$$

in conjunction with

$$|B,R_B;\tilde{h}\rangle = \hat{P}_B(R_B)\hat{D}|A,R_A;\tilde{h}\rangle\eta_h(A,R_A;B,R_B)^{-1} \quad (35)$$

By choosing $\eta_h(A,R_A;B,R_B)$ as a positive number one fixes the relative phases of $|B,R_B;\tilde{h}\rangle$ and $|A,R_A;\tilde{h}\rangle$.

As a further relation we wish to mention

$${}^1/_2\text{trace}((|A,R_A;\tilde{h}\rangle\langle B,R_B;\tilde{h}'| + |B,R_B;\tilde{h}'\rangle\langle A,R_A;\tilde{h}|)\hat{D}) = \delta_{h,h'}\eta_h(A,R_A;B,R_B) \quad (36)$$

that is, hybrid orbitals from different PESHOs do not share electrons.

Nonequivalent Bond Partners *A, B.* The simple applications considered so far have been restricted to electron sharing phenomena between pairs of equivalent atoms. As a consequence we have been content to focus our attention on $\omega_{AB}(r,l_A,m_A;r,l_B,m_B)$, that is, on functions of one continuous variable *r*. If the bond partners *A* and *B* are nonequivalent, it will be safest to consider two-dimensional "electron sharing maps" which would show $\omega_{AB}(r_A,l_A,m_A;r_B,l_B,m_B)$ as contour lines. The data compression from three-dimensional MOs to two-dimensional electron sharing functions is still considerable.

V. The Electronic Structure of PF_5

The electronic structures of hypercoordinate compounds like SF_6 and PF_5 historically have been rationalized by the participation of *3d* orbitals in chemical bonding.[40] An alternative explanation of hypercoordination involves three-center four-electron bonds, for example in the linear $F_{ax}-P-F_{ax}$ subsystem of PF_5.[11] Recent work[41−44] denies the existence of sp^3d hybrids at phosphorus to the point where "the *d* orbital concept is now redundant at best, inaccurate and misleading at worst".[12] The consensus is that PF_5 is a highly ionic compound with some covalent contributions including a three-center four-electron bond.[45]

We will rigorously prove in this section that a delocalized three-center four-electron bond in the linear $F_{ax}-P-F_{ax}$ subsystem of PF_5 does not exist. While we emphasize the importance of ionic bonding, we show that *if* electron sharing is considered, some violation of the octet rule at phosphorus has to be acknowledged. An attempt will be made to reconcile this view with recent work that denies violation of the octet rule.[41−43,46]

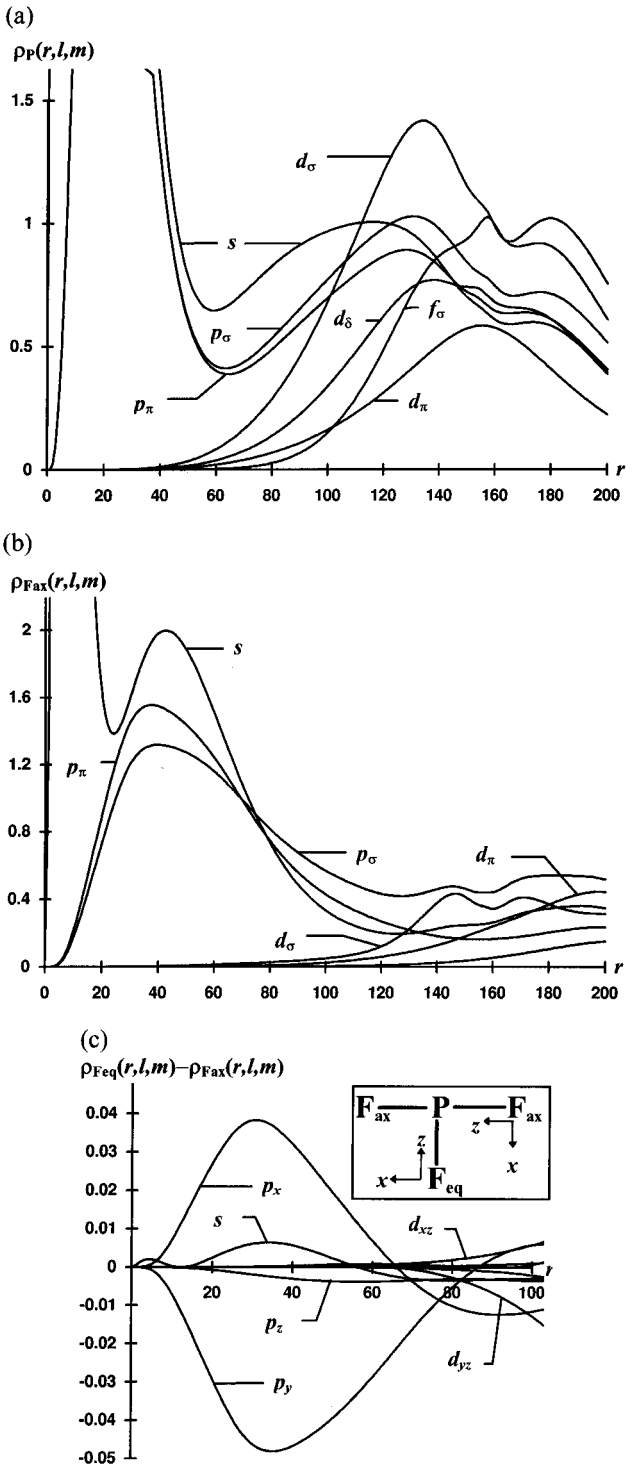

Figure 4. (a) Radial densities $\rho_P(r,l,m)$ of phosphorus in D_{3h}-symmetric PF_5 (SCF/SVP approximation; the bond lengths are $R_{PFeq} = 154$ pm, $R_{PFax} = 157$ pm). p_σ points from phosphorus to an axial fluorine atom. (b) Radial densities $\rho_{Fax}(r,l,m)$ for an axial fluorine atom in PF_5. (c) Difference densities $\rho_{Feq}(r,l,m) - \rho_{Fax}(r,l,m)$ between equatorial and axial fluorine atoms in PF_5.

Atomic Radial Densities in PF_5. Figure 4a shows radial densities of phosphorus in PF_5. The labels σ, π, and δ refer to the linear $F_{ax}-P-F_{ax}$ subsystem. The label F_{ax} (F_{eq}) is meant to refer to the axial (equatorial) fluorine atoms. The calculated

(40) Pauling, L. *The Nature of the Chemical Bond*, 3rd ed.; Cornell University Press: Ithaca, New York, 1960.
(41) Reed, A. E.; Schleyer, P. v. R. *J. Am. Chem. Soc.* **1990**, *112*, 1434.
(42) Magnusson, E. *J. Am. Chem. Soc.* **1990**, *112*, 7940.
(43) Cioslowski, J.; Mixon, S. T. *Inorg. Chem.* **1993**, *32*, 3209.
(44) Cooper, D. L.; Cunningham, T. P.; Gerrat, J.; Karadakov, P. B.; Raimondi, M. *J. Am. Chem. Soc.* **1994**, *116*, 4414.
(45) Kutzelnigg, W. *Angew. Chem., Int. Ed. Engl.* **1984**, *23*, 272.
(46) Reed, A. E.; Weinhold, F. *J. Am. Chem. Soc.* **1986**, *108*, 3586.

(SCF/SVP) bond distances are $R_{PFeq} = 154$ pm and $R_{PFax} = 157$ pm.[47] The maxima of phosphorus p densities at $r \approx 130$ pm, Figure 4a, are buried deep within the valence shells of the fluorine atoms, Figure 4b, giving testimony of high polarity of the PF bonds. The phosphorus p_σ density is slightly larger than the p_π densities since two fluorine atoms (F_{ax}) interact with the $3p_\sigma$ orbital of phosphorus whereas three fluorine atoms (F_{eq}) interact with *two* $3p_\pi$ orbitals. Outside the core region of phosphorus, that is, for $r > 60$ pm, the phosphorus p densities take a position between the s density and the d_σ density. The d_σ density bears little resemblance with the far more diffuse d densities of excited states of isolated phosphorus atoms (not depicted), and a model of bonding build on corresponding spectroscopic sp^3d hybrid orbitals would thus be inappropriate, as is well-known.[42]

Figure 4b shows radial densities $\rho_{Fax}(r,l,m)$ of an axial fluorine atom. The p_σ density at $r = 40-60$ pm is somewhat reduced when compared to the p_π densities, a consequence of the PF_{ax} bond. This reduction in fluorine p_σ density is small when compared to that in F_2, Figure 2b, in agreement with the high degree of bond polarity in PF_5. p_π densities in F_{ax}, Figure 4b, are slightly reduced when compared to those in F_2, Figure 2b. For a rationalization recall that p_π states of fluorine in F_2 tend to share electrons in an antibonding mode, Section III (lone pair repulsion in F_2). In PF_5 no lone pair repulsion exists between F_{ax} and P. In this way fluorine lone pairs are allowed more space in PF_5 than in F_2. An additional cause of the lone pair expansion at F_{ax} would be accumulation of negative charge.

Figure 4c compares radial densities of F_{eq} and F_{ax}. With respect to the σ-type orbitals there is surprisingly little difference, that is, there are no indications that PF_{ax} and PF_{eq} bonds harbour different bonding mechanisms. However, there are differences with respect to the π-type lone pairs at F_{ax} and F_{eq}: the p_y (p_x) lone pair at F_{eq} is more (less) diffuse than the p_π lone pairs at F_{ax}. As a rationalization recall that $F_{eq}PF_{eq}$ bond angles of 120° in the yz plane relieve a p_y lone pair at F_{eq} of repulsion from other fluorine substituents.

Responses of Radial Densities to Structural Changes. Figure 5 shows responses of atomic radial densities in PF_5 upon changes to the bond lengths PF_{ax} and PF_{eq}. Figures 5a and 5b demonstrate only minor differences between $d\rho_P(r,l,m)/dR_{PFax}$ and $d\rho_P(r,l,m)/dR_{PFeq}$. The reduction in phosphorus d_σ densities is slightly more pronounced if an axial fluorine atom is pulled off phosphorus as compared to a situation where an equatorial phosphorus atom is pulled off. s densities show the inverse trend. The involvement of phosphorus d densities is striking, but should not be over-emphasized for the following reasons: (1) In general, responses $d\rho_A(r,l,m)/dR_{AB}$, which relate to "bonds" between heteroatoms A, B, are likely to be strong when electrons in the state $|A;rlm\rangle$ are only loosely bound to A, and thus are easily carried away by B. (2) Significant f densities at phosphorus radii larger than about 90 pm, Figure 4a, indicate that "out there" it may no longer be helpful to speak of phosphorus orbitals because the electronic structure in this regime is more strongly influenced by the potential troughs of the fluorine atoms; what is visible from Figures 5a and 5b for $r \geq 90$ pm is the movement of electronic density bound to fluorine. By the same standards, phosphorus p_σ densities are easily carried away upon stretching of PF bonds. Figure 5c shows that the only significant response in fluorine radial densities to a PF bond stretching motion is depletion of its p_σ density.

Figures 5d−5g display responses in radial densities $d\rho_C(r,l,m)/dR_{AB}$ of atoms C that are not directly involved in the dissociation of some AB bond (A = phosphorus; B, C = fluorine). In PF_5 these responses are on average one order of magnitude smaller than the direct responses $d\rho_B(r,l,m)/dR_{AB}$. In the presence of a three-center four-electron bond between the two axial fluorine atoms (F_{ax} and F_{ax}') and phosphorus, one would intuitively expect a comparatively strong response in radial densities of F_{ax} when the PF_{ax}' bond is stretched. On the contrary, this indirect response is the weakest of all indirect responses, Figures 5d−5g. There is, however, comparatively strong coupling between p_σ densities at axial (equatorial) fluorine atoms and the stretching of a PF_{eq} (PF_{ax}) bond, Figure 5e,f. An understanding of these effects will emerge later.

Phosphorus Hypervalence in PF_5. Figures 4a and 5a,b gave testimony of non-negligible d densities of phosphorus at radii larger than 50 pm. From these data it is not clear whether d functions at phosphorus are merely polarizing the phosphorus valence shell or are of hypervalent character. For example, the most conspicuous phosphorus d_σ density in Figure 4a (recall that the label σ is meant to refer to the linear $F_{ax}-P-F_{ax}$ subsystem) could result from admixture of a d_σ function to the phosphorus $3s$ orbital. The occupancies of the atomic neighborhood natural orbitals (ANNOs) of phosphorus in PF_5, Table 2, show that on the contrary, practically all of the d_σ population of phosphorus at radii between 50 and 90 pm is hypervalent in character, and concentrated in the ANNO labeled $3d_{z^2}$. According to the population ratios in Table 2 there is no clear distinction between the four valence ANNOs and the (hypervalent) $3d_{z^2}$ ANNO. Notable is the relatively high s population.

Structural effects of d function participation, here related to phosphorus hypervalence in PF_5, are often probed by deleting d-type basis functions (from phosphorus), and by subsequent reoptimization of the molecular structure. Since this approach uncontrollably introduces basis set superposition errors, we use it only as a starting point for further consideration. In the SCF/SVP approximation applied to PF_5 one has $\rho_P(r,d_{z^2}) = 0.8$ for $r = 60$ pm (z direction aligned with C_3 symmetry axis), the equilibrium structure constants being $R_{PFax} = 157$ pm and $R_{PFeq} = 154$ pm. These characteristics change to $\rho_P(60\text{pm},d_{z^2}) = 0.3$, $R_{PFax} = 159$ pm, and $R_{PFeq} = 154$ pm, if the phosphorus d_{z^2} basis function is deleted from the SVP basis set. In an effort to reduce the influence of basis set superposition errors on structure parameters while maintaining an electronic structure which largely forbids a significant d_{z^2} population near phosphorus, the electronic and molecular structure of PF_5 has subsequently been optimized subject to the constraint $\rho_P(60\text{pm},d_{z^2}) = 0.3$, using the original SVP basis set. This led to $R_{PFax} = 164$ pm and $R_{PFeq} = 155$ pm.[48] Quite obviously the structural effects of phosphorus d_{z^2} participation appear to become significantly stronger as soon as basis set superposition effects inherent in basis function deletion procedures are largely eliminated. By the way, the constraint $\rho_P(r,d_{z^2}) = 0.3$ for $r = 60$ pm raises the energy of PF_5 by 101 kJ/mol.

On a per bond basis, the energetic effects of phosphorus d-type basis functions are not *much* larger in PF_5 than in PF_3.[42,49] To be explicit, we follow Magnusson[42] and view phosphorus d function participation in PF_3 as a characteristic of PF bonds that is transferable to PF_5. Under this premise one can estimate a d-related stabilization energy of phosphorus in PF_5 by multiplying the corresponding d-related stabilization energy in

(47) Respective experimental values are 153 and 158 pm.

(48) We wish to mention that under these constraints $\omega_{FaxFax'}(r_{max},p_\sigma\ r_{max},p_\sigma) = 0.041$. Breaking of D_{3h} symmetry has not been considered.

(49) We would like to caution readers about energetic effects of d-type basis functions as analyzed in ref 44. In ref 44 sets of six Cartesian d functions are used, that is, their deletion from the basis set involves the removal of an s-type basis function. This forbids conclusions that subsequently obtained energy differences are d effects.

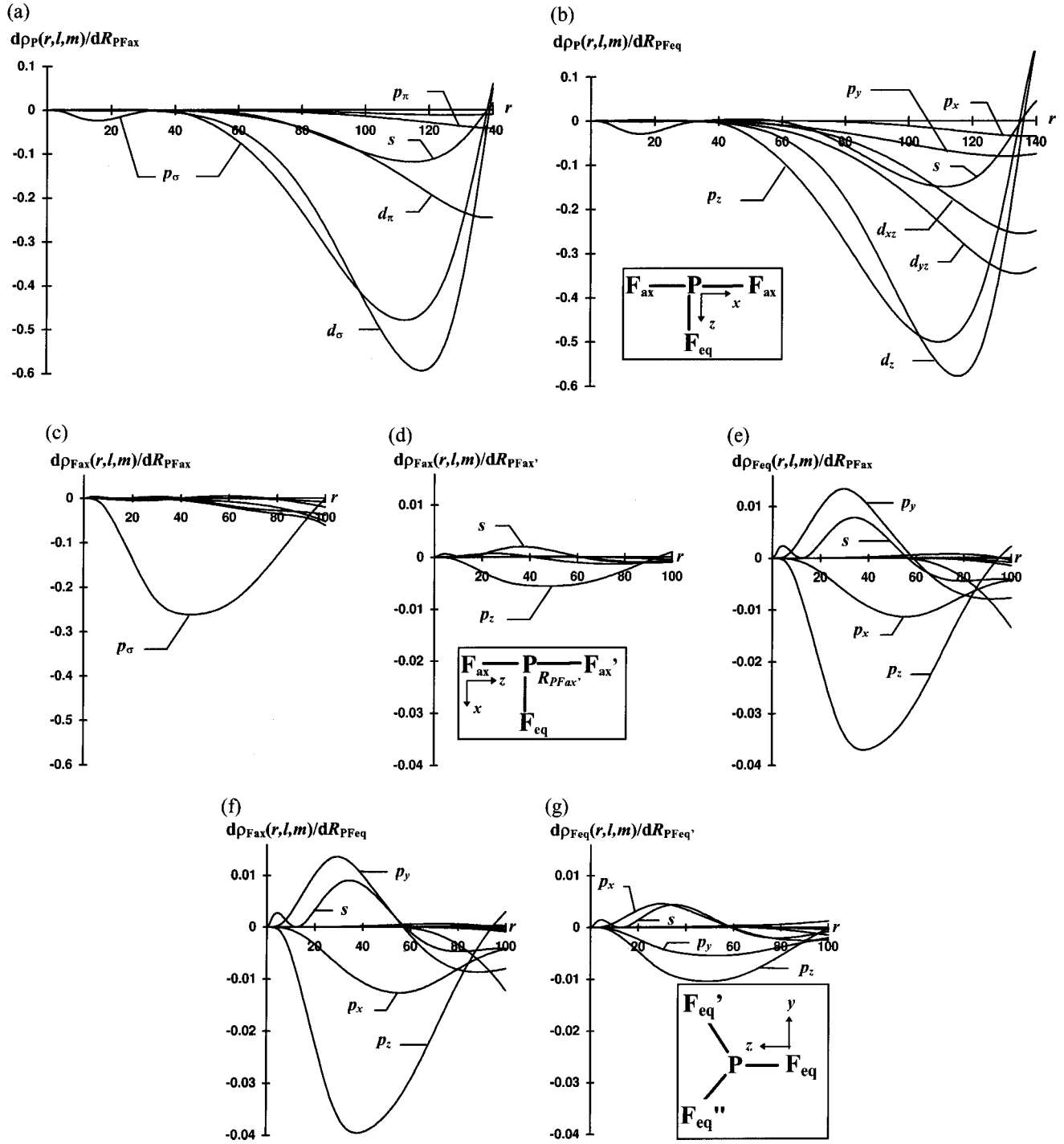

Figure 5. Responses of radial densities of atoms in PF_5 to changes in bond lengths R_{PFax} or R_{PFeq}. Each time only one of the PF_{ax} or PF_{eq} bonds is stretched. Cartesian reference frames are specified in the insets where necessary. For parts e and f the reference frames given in Figure 4c apply.

PF_3 by 5/3. Such an extrapolation underestimates *d*-related stabilization in PF_5 by 58 kJ/mol[50] or more,[51] that is, a factor of 2 would be more appropriate than a factor of 5/3. These energies are in harmony with *d* populations $N_P(R,l=2)$ that are about a factor of 2 larger in PF_5 than in PF_3. ANNO analysis applied to the phosphorus atom in PF_3 shows a much reduced hypervalent population in this compound as compared to the situation in PF_5, cf. Tables 2 and 3.

(50) *d*-type basis functions have been omitted from phosphorus only, but otherwise the SCF/SVP description is maintained. As a result of the deletion of a single *d* shell the total energy of PF_5 rises by 454 kJ/mol, that of PF_3 by 238 kJ/mol.

(51) From ref 42 one infers 100 kJ/mol; in that case the basis set at fluorine did not include polarization functions.

No Three-Center Four-Electron Bond in PF_5. It has long been suspected that the linear $F_{ax}-P-F_{ax}'$ subsystem in D_{3h}-symmetric PF_5 exhibits characteristics of a three-center four-electron bond.[11,12,45] Now, an indispensable characteristic of chemical bonding is electron sharing (electronic coherence) between its participating atoms. In case of a three-center four-electron bond of the general type $B-A-B'$ such electron sharing should also occur between atomic states at B and B', i.e., between $|B;rlm\rangle$ and $|B';r'lm\rangle$, as otherwise one could hardly speak of a delocalized system. The absence of such delocalization may rigorously be proven by showing that $|\omega_{BB'}(r,l,m;r',l,m)|$ is near-zero for all reasonable values of r and r'.[52] It turns out that a well-defined maximum of $|\omega_{BB'}(r,l,m;r',l,m)|$

Table 2. Atomic Neighborhood Natural Orbitals (ANNOs) $|P,R;\alpha\rangle$ of Phosphorus in PF_5 (SCF/SVP)[a]

α	*l*,*m*[b]	10	20	30	40	50	60	70	80	90	100
3s	*s*	0.0000	0.0000	0.0021	0.0154	0.0551	0.1315	0.2445	0.3871	0.5504	0.7265
	d_{z^2}	0.0000	0.0000	0.0000	0.0000	0.0000	0.0000	0.0001	0.0002	0.0003	0.0003
	3,3	0.0000	0.0000	0.0000	0.0000	0.0000	0.0000	0.0002	0.0008	0.0026	0.0073
	4,0	0.0000	0.0000	0.0000	0.0000	0.0000	0.0000	0.0000	0.0002	0.0011	0.0038
$3p_y$	p_y	0.0000	0.0000	0.0010	0.0060	0.0212	0.0534	0.1071	0.1836	0.2813	0.3969
	d_{xy}	0.0000	0.0000	0.0000	0.0001	0.0007	0.0024	0.0064	0.0147	0.0305	0.0584
	3,−1	0.0000	0.0000	0.0000	0.0000	0.0000	0.0000	0.0001	0.0005	0.0017	0.0048
$3p_z$	p_z	0.0000	0.0000	0.0011	0.0066	0.0232	0.0586	0.1179	0.2030	0.3133	0.4467
	3,0	0.0000	0.0000	0.0000	0.0000	0.0000	0.0001	0.0005	0.0018	0.0057	0.0156
$3d_{xy}$	p_y	0.0000	0.0000	0.0000	0.0000	0.0000	0.0002	0.0006	0.0018	0.0045	0.0100
	d_{xy}	0.0000	0.0000	0.0000	0.0003	0.0015	0.0046	0.0111	0.0225	0.0401	0.0647
	3,−1	0.0000	0.0000	0.0000	0.0000	0.0000	0.0000	0.0000	0.0001	0.0003	0.0009
$3d_{xz}$	d_{xz}	0.0000	0.0000	0.0000	0.0003	0.0012	0.0038	0.0093	0.0193	0.0357	0.0609
	3,2	0.0000	0.0000	0.0000	0.0000	0.0000	0.0000	0.0000	0.0002	0.0005	0.0015
$3d_{z^2}$	d_{z^2}	0.0000	0.0000	0.0001	0.0013	0.0052	0.0158	0.0383	0.0800	0.1497	0.2570
	3,3	0.0000	0.0000	0.0000	0.0000	0.0000	0.0000	0.0003	0.0012	0.0038	0.0100
	4,0	0.0000	0.0000	0.0000	0.0000	0.0000	0.0000	0.0000	0.0001	0.0004	0.0015

[a] Each ANNO is characterized by its partial populations $n_\alpha(P,R,l,m)$, eq 19, for $R = 10, 20, ..., 100$ pm (numbers are truncated after four postdecimal digits). Symmetry-redundant orbitals (p_x, d_{yz}, and $d_{x^2-y^2}$ are symmetry-equivalent to p_y, d_{xz}, and d_{xy}, respectively) and core orbitals have been omitted. The bond distances are $R_{PFax} = 157$ pm and $R_{PFeq} = 154$ pm. [b] $F_{ax}-P-F_{ax}$ on the *z* axis.

Table 3. Atomic Neighborhood Natural Orbitals (ANNOs) $|P,R;\alpha\rangle$ of Phosphorus in PF_3 (SCF/SVP)[a]

α	*l*,*m*[b]	10	20	30	40	50	60	70	80	90	100
3s	*s*	0.0000	0.0001	0.0032	0.0231	0.0819	0.1914	0.3453	0.5261	0.7147	0.8969
	p_z	0.0000	0.0001	0.0006	0.0030	0.0101	0.0251	0.0494	0.0818	0.1182	0.1525
	d_{z^2}	0.0000	0.0000	0.0000	0.0000	0.0000	0.0001	0.0002	0.0004	0.0006	0.0009
$3p_y$	p_y	0.0000	0.0001	0.0008	0.0044	0.0155	0.0390	0.0782	0.1343	0.2061	0.2916
	d_{xy}	0.0000	0.0000	0.0000	0.0001	0.0004	0.0014	0.0036	0.0080	0.0164	0.0310
	d_{yz}	0.0000	0.0000	0.0000	0.0002	0.0009	0.0028	0.0070	0.0151	0.0293	0.0526
	3,−2	0.0000	0.0000	0.0000	0.0000	0.0000	0.0000	0.0002	0.0006	0.0020	0.0057
$3p_z$	*s*	0.0000	0.0000	0.0002	0.0008	0.0027	0.0072	0.0156	0.0289	0.0472	0.0695
	p_z	0.0000	0.0000	0.0010	0.0062	0.0219	0.0547	0.1080	0.1821	0.2750	0.3846
	d_{z^2}	0.0000	0.0000	0.0000	0.0000	0.0000	0.0000	0.0001	0.0003	0.0006	0.0014
	3,0	0.0000	0.0000	0.0000	0.0000	0.0000	0.0000	0.0002	0.0006	0.0018	0.0048
	3,3	0.0000	0.0000	0.0000	0.0000	0.0000	0.0001	0.0002	0.0008	0.0024	0.0064
$3d_{xy}$	p_y	0.0000	0.0000	0.0000	0.0000	0.0000	0.0001	0.0002	0.0005	0.0014	0.0035
	d_{xy}	0.0000	0.0000	0.0000	0.0002	0.0009	0.0026	0.0063	0.0131	0.0238	0.0395
	d_{yz}	0.0000	0.0000	0.0000	0.0000	0.0000	0.0001	0.0002	0.0004	0.0007	0.0012
	3,−2	0.0000	0.0000	0.0000	0.0000	0.0000	0.0000	0.0002	0.0006	0.0018	0.0046
$3d_{yz}$	p_y	0.0000	0.0000	0.0000	0.0000	0.0000	0.0001	0.0002	0.0006	0.0014	0.0028
	d_{yz}	0.0000	0.0000	0.0000	0.0001	0.0003	0.0009	0.0021	0.0044	0.0079	0.0131
	3,−2	0.0000	0.0000	0.0000	0.0000	0.0000	0.0000	0.0001	0.0003	0.0007	0.0015
	3,−1	0.0000	0.0000	0.0000	0.0000	0.0000	0.0000	0.0002	0.0006	0.0018	0.0045
$3d_{z^2}$	*s*	0.0000	0.0000	0.0000	0.0000	0.0000	0.0000	0.0000	0.0001	0.0002	0.0005
	p_z	0.0000	0.0000	0.0000	0.0000	0.0000	0.0000	0.0000	0.0001	0.0002	0.0007
	d_{z^2}	0.0000	0.0000	0.0000	0.0002	0.0007	0.0022	0.0053	0.0110	0.0205	0.0348
	3,0	0.0000	0.0000	0.0000	0.0000	0.0000	0.0000	0.0001	0.0002	0.0006	0.0014
	3,3	0.0000	0.0000	0.0000	0.0000	0.0000	0.0000	0.0002	0.0006	0.0016	0.0040

[a] Each ANNO is characterized by its partial populations $n_\alpha(P,R,l,m)$, eq 19, for $R = 10, 20, ..., 100$ pm (numbers are truncated after four postdecimal digits). Symmetry-redundant orbitals and core orbitals have been omitted. The bond distance is $R_{PF} = 157$ pm. [b] *z* axis is symmetry axis; *xz* plane is mirror plane.

is attained at some radius $r_{max} = r = r'$, close to where $\rho_B(r,l,m)$ has its maximum (this holds in our applications, Table 4, where *B* and *B*′ are symmetry-equivalent atoms of some electronegative element). In Table 4 we compare $\omega_{BB'}(r_{max},l,m;r_{max},l,m)$ for a number of prototypical systems. As expected, electron sharing between *B* and *B*′ shows up in the σ system of KrF_2 or in the π system of CO_2, Table 4. Similar, albeit less significant, is electron sharing among p_π states at fluorine atoms in BF_3, giving testimony of weak Y-conjugation in that system (the degree of electron sharing is relatively small due to high polarity of BF π bonds). In the hypothetical molecule NF_5, constrained to point-group symmetry D_{3h}, the same hallmarks of a three-center four-electron bond can be found in the linear $F_{ax}-N-F_{ax}'$ subsystem as in KrF_2 or CO_2. Amazingly, virtually no delocalization of this kind can be detected for the linear $F_{ax}-P-F_{ax}'$ subsystem in PF_5, Table 4. This result holds for the simple SCF/SVP method of calculation, but is also true when the basis set is further expanded, or when the B3LYP density functional is utilized.[53] A similar result, though not quite as clear-cut, is obtained for SF_6.

In principle it is possible that the sole reason for the absence of three-center four-electron bonding in PF_5 is an extremely high polarity of the PF bonds. For example, the somewhat more covalent compound PCl_5 exhibits minor signs of delocalization within the linear $Cl_{ax}-P-Cl_{ax}'$ subsystem, Table 4. To contradict a purely ionic explanation let us delete *d*-type basis functions at phosphorus in PF_5. $\omega_{FaxFax'}(r_{max},p_\sigma;r_{max},p_\sigma)$ then

(52) In general some consideration will have to be given to the possibility of choosing *l*,*m* differently for *B*,*B*′. In our applications these choices are so obvious that we do not elaborate on that issue.

(53) We are not aware of a physically sound basis that would justify the evaluation of non-local one-electron properties simply from Kohn−Sham orbitals. Nevertheless, the numbers presented in Table 3 for the B3LYP density functional have been obtained as if the operator $\hat{O}_{BB'}$ were a local one-electron operator. Such an "uncoupled" approximation usually forms the basis of any discussion of electronic structure in terms of orbitals within the framework of density functional theory.

Table 4. Electron Sharing Function $\omega_{BB'}(r_{max},l,m;r_{max},l,m)$ of Two Nonbonded Atoms B,B' in Molecules $ABB'C_n$ That Contain a Linear $B-A-B'$ Subsystem (Exception: BF_3)

molecule	method	AB[a]	AC[a]	$B-A-B'$	l,m[b]	r_{max}[c]	$\omega_{BB'}(r_{max},l,m;r_{max},l,m)$
CO_2	SCF/SVP	113.7		O−C−O	p_π	42	−0.238
BF_3	SCF/SVP	129.8		F−B−F	p_π	36	−0.093
KrF_2	SCF/SVP	182.5		F−Kr−F	p_σ	36	0.304
NF_5	SCF/SVP	154.5	131.1	F−N−F	p_σ	36	0.225
PF_5	SCF/SVP	157.3	154.1	F−P−F	p_σ	45	0.012
	SCF/SVp[d]	e	e			39	0.029
	SCF/TZV2d1f	156.0	151.9			30	0.007
	B3LYP/SVP	160.0	157.5			30	0.004
	B3LYP/TZV2d1f	159.4	155.8			24	0.002
PCl_5	SCF/SVP	214.7	203.4	Cl−P−Cl	p_σ	72	0.066
	SCF/SVp[d]	e	e			75	0.096
SF_6	SCF/SVP	154.8		F−S−F	p_σ	37	0.037
	SCF/SVp[d]	e	e			37	0.074

[a] Calculated equilibrium bond distance in pm. [b] p_π refers to Cartesian p functions at B and B' oriented perpendicularly to the $B-A-B'$ subsystem; p_σ is oriented toward A. [c] r_{max} is the radius at which the electron sharing function $|\omega_{BB'}(r_{max},l,m;r_{max},l,m)|$ attains its maximum. [d] SCF/SVP basis set with d-type basis functions omitted at A. [e] SCF/SVP equilibrium geometry.

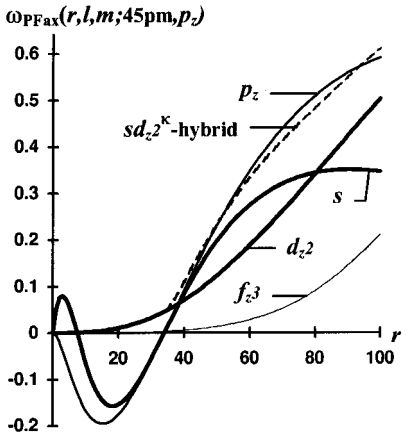

Figure 6. Degree of electron sharing $\omega_{PFax}(r,l,m;r_{Fax},p_z)$ between one-electron states $|P;r,l,m\rangle$ at phosphorus and a p_z state $|F_{ax};r_{Fax},p_z\rangle$ at one of the axial fluorine atoms. The radius r_{Fax} is held fixed at 45 pm. The radius r is varied between 0 and 100 pm (abszissa). Local Cartesian coordinate frames are fixed to both atoms with z axes pointing head on.

rises from 0.012 (the SCF/SVP result) to 0.029 (the result labeled SCF/SVp in Table 4),[54] that is, the characteristic delocalization of a three-center four-electron bond involving the p_σ orbitals of the axial fluorine ligands is partially re-established.

Toward a Consistent Interpretation of Bonding in PF_5. It has become evident that bonding in PF_5 may not be regarded as purely ionic, does not involve (spectroscopic) sp^3d hybrids at phosphorus (even though hypervalent interactions are non-negligible), and cannot be explained by a three-center four-electron bond model. To obtain a positive description it is helpful to consider the electron sharing function $\omega_{PFax}(r,l,m;r',p_\sigma)$ of one-electron states $|P;rlm\rangle$ centered at phosphorus and p_σ states centered at F_{ax}, Figure 6. On the side of fluorine (F_{ax}) we restrict our analysis to a fixed radius, here $r' = 45$ pm; results obtained for other reasonable choices of r' are basically identical. As it turns out, for phosphorus radii 20 pm $\leq r \leq$ 50 pm one has $\omega_{PFax}(r,s;r',p_\sigma) \approx \omega_{PFax}(r,p_\sigma;r',p_\sigma)$. At larger radii, 50 pm $\leq r \leq$ 80 pm, there is an increasing contribution from $\omega_{PFax}(r,d_\sigma;r',p_\sigma)$ so that $\omega_{PFax}(r,d_\sigma;r',p_\sigma)^2 + \omega_{PFax}(r,s;r',p_\sigma)^2 \approx \omega_{PFax}(r,p_\sigma;r',p_\sigma)^2$. The square root of the left-hand side is depicted as a dashed line in Figure 6. The rather good approximation of $\omega_{PFax}(r,p_\sigma;r',p_\sigma)$ by this dashed line is the primary reason (on the covalent side) for the absence of a delocalization fingerprint from three-center four-electron bonding in the linear $F_{ax}-P-F_{ax}'$ subsystem. Obviously the participation of a phosphorus $3s$-type orbital is more important for electron sharing between phosphorus and the axial fluorines than the participation of a $3d_\sigma$-type orbital.

The strong involvement of a phosphorus $3s$-type orbital in PF_{ax} bonding (partially by forming a hybrid with a $3d_\sigma$ state) implies two alternative consequences: (1) delocalization between p_σ states of axial fluorine atoms F_{ax} on one side and p_σ states of equatorial fluorine atoms F_{eq} on the other side; and (2) participation of a phosphorus $3d_\sigma$-type orbital in covalent interactions between P and F_{eq}. While point 2 holds to some degree, as may be demonstrated by a comparison of Figures 5a and 5b, it is also clear from these figures that phosphorus $3d_\sigma$ participation in covalent interactions between P and F_{eq} is somewhat smaller than that between P and F_{ax}. Thus it is not surprising that significant delocalization between p_σ states at F_{ax} and F_{eq} is detected in PF_5: $\omega_{FaxFeq}(r_{max},p_\sigma;r_{max},p_\sigma) = -0.130$ for $r_{max} = 36$ pm (note that p_σ here corresponds to a Cartesian p function at fluorine that is pointed toward phosphorus). This finding not only is in agreement with the ratios between ANNO populations, Table 2, but it also explains why $d\rho_{Feq}(r,p_z)/dR_{PFax}$, Figure 5e, and $d\rho_{Fax}(r,p_z)/dR_{PFeq}$, Figure 5f, have larger magnitudes than $d\rho_{Fax}(r,p_z)/dR_{PFax'}$, Figure 5d (note again that the local z direction at each fluorine atom has been chosen so that $p_z = p_\sigma$ is oriented toward P).

Discussion. We discuss our results on bonding in PF_5 in the light of recent publications from other workers. The high bond polarity in PF_5 is a rather well-established fact that has most recently been re-emphasized by Cioslowski et al.[43] As a consequence of a formal phosphorus charge of 3.37 Cioslowski et al. count only 1.63 valence electrons at phosphorus and conclude that the octet rule at phosphorus is not violated. This is a dangerous conclusion. For example, if we look at a neighborhood of phosphorus in PF_5 that accommodates 1.63 valence electrons (a radius between 80 and 90 pm would be appropriate), we find little comfort in neglecting the hypervalent $3d_{z^2}$ population as it is of the same magnitude as the $3p_x$ population, Table 2.[55]

(54) Practically the same result is obtained, if the d_σ basis function only is deleted at phosphorus, but this is not too surprising in view of the phosphorus ANNOs, Table 2, or in view of phosphorus radial densities, Figure 4a.

(55) Even if fewer than eight valence electrons are counted in some neighborhood of an atomic nucleus (formally by calculating the *trace* of a projected one-electron density operator), it may still be impossible—even in an approximate sense—to accommodate them in four (space) orbitals—a situation that arises in PF_5. In that case a *sum* of seemingly less than 8 electrons refers to fractional contributions from *more* than 8 different electrons, and the octet rule is violated.

Our investigation is in harmony with recent results by Cooper et al.[44] in that all of the PF bonds in PF_5 look largely the same, and this contradicts claims of localized *pd* hybrids in the linear $F_{ax}-P-F_{ax}$ subsystem as well as the three-center four-electron bond model (the latter point is not addressed by Cooper et al.).

Reed and Weinhold[46] previously have emphasized the importance of central atom *s* orbital involvement in covalent bonding in SF_6. They also found that "the qualitative influence of *d* orbitals ... in stabilizing hypervalent compounds ... cannot be neglected".[46] Kutzelnigg has come to similar conclusions before.[45] Needless to say we agree.

Reed and Schleyer[41] write: "The role of *d* functions in hypervalent molecules is to provide orbital space at the central atom to accept electronic charge from the ligands." According to this view hypervalent *d* populations may be regarded as parked in a neighborhood of phosphorus without much energy gained or expended. Qualitatively this is nicely confirmed when a fluorine atom is pulled off PF_5, Figures 5a and 5b: First of all the phosphorus d_σ density is reduced, subsequently the phosphorus p_σ density (if seen in comparison to the static densities, Figure 4a), and to a lesser degree the phosphorus *s* density.

If one likes to think of a potential trough for *d* electrons near phosphorus in PF_5, then Figures 4a and 5a,b tell that it must be shallower than a corresponding trough for valence *p* electrons, etc. In the case of the compound $P(NH_2)_4^+$ we have thoroughly pursued this line of thought.[56] We represented the phosphorus core electrons by an effective core potential,[57] and added the spherically averaged Coulomb potential and the centrifugal potential $l(l + 1)/(2r^2)$. The resulting effective one-electron potential for valence *s* electrons displays a trough at $r \approx 60$ pm, a more shallow trough for valence *p* electrons, yet no trough for *d* electrons. *d* electrons would experience only a level potential at radii between 50 and 90 pm from phosphorus and would neither be strongly bound nor dispelled. First-row atoms exert a fairly repulsive effective potential onto *d* electrons.[56,58] As there seems to be no potential trough for *d* electrons in the neighborhood of phosphorus (in phosphorus compounds), it seems justified to reject the entire concept of phosphorus *d* orbital involvement in chemical *bonding*, cf. Magnusson.[42] While there is a continuous transition between covalent bonding on one hand and weaker electron sharing interactions on the other hand, it is necessary to use different qualifiers at some point of such a transition.

There is some disagreement between our notion of hypervalence in PF_5 and that of other workers who have previously concluded that the octet rule is not violated.[41,42] It is implicit to partitioning techniques used in population analyses that locally hypervalent populations are reduced by some mapping onto other atoms. A particularly transparent example in this respect is the generalized atomic polar tensor approach applied by Cioslowski.[8] In the latter approach it is not so much important at which location electronic structure resides, but how it is correlated with movements of atoms.

In contrast, in this work we took a *local point of view*, and found that the electronic structure surrounding the phosphorus nucleus in PF_5 is not well describable in terms of four orbitals (for simplicity we ignore core electrons). A description involving a fifth occupied orbital of (locally) d_{z^2}-type appears equally appropriate, Table 2, even though this means violation of the octet rule. Efforts to preserve the octet rule by a partial suppression of the phosphorus d_{z^2} population imply non-negligible corrections to the energetic stability[59] and to the molecular structure of PF_5. Nevertheless, the hypervalent d_{z^2} population is rather weakly bound to phosphorus, and its participation in covalent interactions with the fluorine ligands should not be qualified as covalent bonding, in particular, as a potential well for the the d_{z^2} population appears to be missing. The relative ease with which the phosphorus d_{z^2} population is depleted indicates that a different view of atoms in molecules—one which partitions molecular electronic structure according to its correlation with nuclear movements—may well confirm the octet rule for phosphorus in PF_5.

VI. Conclusion

In chemistry the analysis of molecular electronic structure in terms of *s*, *p*, *d*, ... functions of a participating atom is generally acknowledged. From quantum mechanics it is known that most physical properties will not be compatible with the corresponding angular momentum operators. One property which is compatible with angular momentum is radius or any function thereof. In this way the willingness to speak of atomic angular momentum eigenfunctions implies a restriction to *spherical* atomic neighborhoods (characterized, e.g., by radius and origin). By scanning through a complete set of neighborhoods of a given atom, the surrounding molecular electronic structure may be featured by functions of radius from an otherwise unbiased atomic point of view. These functions may serve as a first-principles basis of a comparison between atoms in molecules. Among them are radial densities/populations of electrons with specific angular momenta, their responses to changes in molecular structure, as well as measures to what extent the one-particle density matrix can locally be described in terms of core and valence orbitals, Sections II and III. Phenomena like covalent bonds and electronic delocalization, that by definition are not attributable to a single atom, are characterized on an equal footing by probing the degree of electron sharing between angular momentum eigenstates contained in atomic neighborhoods of different atoms, Section III. It has been outlined how this line of thought leads to a concept of hybrid orbitals in chemical bonding with no other ingredients than principles of quantum mechanics and spherical atomic neighborhoods.

The proposed approach is not a black box method as it requires careful interpretation. For example, nothing has been built into the approach that would tell beyond which maximum size it is no longer useful to consider atomic neighborhoods. Fortunately this information is signaled by the molecular system under scrutiny by the emergence of high angular momentum

(56) Häser, M. Manuscript in preparation.

(57) Kahn, L. R.; Baybutt, P.; Truhlar, D. G. *J. Chem. Phys.* **1976**, *65*, 3826.

(58) Nevertheless, even compounds of first-row elements may exhibit (small) hypervalent *d* populations and, moreover, non-negligible stabilization energies that relate to *d*-type basis functions, cf. ref 42. We do not think that this is merely an artefact of a mathematical description based on atom-centered basis functions. We offer the following explanation (see also: Cruickshank, D. W. J. *J. Mol. Struct.* **1985**, *130*, 177): "Inert" orbitals like lone pairs, when they extend to some other atom in a molecule, may no longer decay unperturbed and exponentially into the infinite. They try to avoid energy penalties brought about by othogonality constraints. This can be achieved by populating those angular momentum eigenfunctions at the other atom that do not relate to its occupied orbitals. This process may become important well before such angular momentum eigenfunctions at the other atom are sufficiently low in energy for a covalent bond to form. If we disfavor this possibility, for example, by omission of *d*-type basis functions, or, more directly, by applying constraints on *d* densities, then the total energy is bound to rise. Note again that a continuous transition from this type of behavior toward "genuine" bond formation exists; the level radial potential of *d* electrons in phosphorus probably is intermediate in this transition.[56]

(59) In addition to the results about PF_5 note that *d*-type basis functions offer the crucial extra stabilization needed to stabilize SF_6 against dissociation, cf.: Magnusson, E. *J. Am. Chem. Soc.* **1993**, *115*, 1051. ANNO analysis indicates a dominantly hypervalent *d* population at sulfur.

populations. The latter demarcate outer limits to atomic thinking in molecules.

So far all applications have rested on single determinant approaches using atom-centered basis functions. This is a consequence of implementational limitations. The analytic tools proposed are applicable to any kind of approximation of molecular electronic structure for which the one-particle density operator can be constructed.

Some of the applications presented would benefit from an inclusion of electronic correlation in the approximation of their electronic structures. Most of all, this applies to F_2, KrF_2, and probably NF_5. In these compounds it may be expected that one-particle delocalization phenomena that appear strong in the self-consistent field approximation are partly replaced by correlation phenomena. However, our discussion of phosphorus pentafluoride (PF_5) will hardly be invalidated.

The analysis of the electronic structure of PF_5, Section V, illustrates how the proposed methods go together to produce a coherent picture of bonding. An astonishing discovery is the absence of electron sharing between p_σ orbitals at axial fluorine atoms. As there is no three-atom delocalization in the system $F_{ax}-P-F_{ax}$, one should not speak of a three-center four-electron bond, and the picture of such a bond together with localized two-center two-electron bonds between equatorial fluorine atoms (F_{eq}) and phosphorus is wrong. This result is largely a consequence of strong phosphorus *3s* participation in covalent bonding with p_σ orbitals from all five fluorine atoms. A further consequence of this *3s* effect is electronic delocalization between axial and equatorial fluorine atoms, also manifest in responses of densities at F_{ax} (F_{eq}) to perturbations [bond stretching] regarding F_{eq} (F_{ax}). Any residual delocalization left between axial fluorine atoms disappears as soon as hypervalence effects involving a $3d_{z^2}$ orbital at phosphorus are accounted for. No reference is made to the diffuse spectroscopic *3d* orbital of an isolated phosphorus atom; rather the precise meaning of $3d_{z^2}$ involvement is as follows. If in the spatial neighborhood of phosphorus electronic structure is represented by as few orbitals as possible, one finds besides core and four normal valence orbitals yet another significantly populated orbital of local $3d_{z^2}$ character. This orbital population is depleted preferentially when a fluorine atom is pulled off PF_5. Probably it is not held in place by a potential trough at or near phosphorus (up to radii of 100 pm),[56] but its form and existence is caused by donation from the ligands and by the reluctance of phosphorus to dispel it. This form of electron sharing implies only a moderate stabilization. While this wording tends to emphasize some qualitative difference between the (local) $3d_{z^2}$ orbital and normal valence orbitals at phosphorus it should be clear that the different behavior of valence *s*, valence *p*, and the hypervalent $3d_{z^2}$ populations merely marks signposts of an otherwise continuous transition between covalent bonding on one side and weaker electron sharing interactions on the other.

FORTRAN Code. A FORTRAN source code for the calculation of matrix elements $\langle A;rlm|\nu\rangle$, where $|\nu\rangle$ is a linear combination (contraction) of Cartesian Gaussfunctions, is available via ftp (file transfer protocol) at internet address "ftp.chemie.uni-karlsruhe.de" with login-ID "anonymous" in the directory "pub/OCE/FORTRAN".

Acknowledgment. We thank Professor R. Ahlrichs and Dr. J. Gauss for valuable discussions and comments on the manuscript. Financial support came from the Deutsche Forschungsgemeinschaft (Ha 2127/1-1).

JA953109T